

Effect of topological defects and Coulomb charge on the low energy quantum dynamics of gapped graphene

Baishali Chakraborty,^{1,*} Kumar S. Gupta,^{1,†} and Siddhartha Sen^{2,‡}

¹*Theory Division, Saha Institute of Nuclear Physics, 1/AF Bidhannagar, Calcutta 700064, India*

²*CRANN, Trinity College Dublin, Dublin 2, Ireland*

(Dated: September 14, 2021)

We study the combined effect of a conical topological defect and a Coulomb charge impurity on the dynamics of Dirac fermions in gapped graphene. Beyond a certain strength of the Coulomb charge, quantum instability sets in, which demarcates the boundary between sub and supercritical values of the charge. In the subcritical regime, for certain values of the system parameters, the allowed boundary conditions in gapped graphene cone can be classified in terms of a single real parameter. We show that the observables such as local density of states, scattering phase shifts and the bound state spectra are sensitive to the value of this real parameter, which is interesting from an empirical point of view. For a supercritical Coulomb charge, we analyze the system with a regularized potential as well as with a zigzag boundary condition and find the effect of the sample topology on the observable features of the system.

I. INTRODUCTION

The dynamics of Dirac fermions in a 2+1 dimensional conical space-time [1] or in the presence of a cosmic string [2] exhibits a variety of rich nonperturbative quantum features. In spite of strong theoretical interest, the quantum properties of such 2D fermionic systems are difficult to observe in the laboratory. The experimental fabrication of monolayer graphene in 2004 [3–5], whose low energy excitations behave like negatively charged fermions satisfying a two dimensional Dirac equation [6–12], offers new possibilities to study the effect of topological defects in such lower dimensional fermionic systems [13–32]. The Dirac type excitations in pristine graphene are gapless. However, various impurities, electron-electron interactions, substrate structures and other short distance effects can violate the sublattice symmetry in graphene, leading to a mass gap which has attracted both theoretical [33–43] and experimental [44–50] attention. Thus, the gapped graphene system provides a unique template to study the nonperturbative quantum features of massive Dirac fermions in the presence of a topological defect.

In graphene the Fermi velocity $v_F \approx 10^6 m/s$, which is approximately 300 times smaller than the velocity of light. Consequently, a relatively small external Coulomb charge impurity $Ze \sim 1$ leads to strong nonperturbative electric field effects in graphene [36, 51–65]. In a gapped graphene system, the external Coulomb charge is said to reach the critical value when the system dives into the negative energy continuum [58, 61, 64] and quantum instability sets in. Any given external charge in gapped graphene can therefore be classified as either sub or super critical. These two different regimes are characterized by markedly different behaviour of the observables such as the local density of states (LDOS) [58].

In this paper we shall study the combined effect of a conical topological defect and an external Coulomb charge impurity on the low energy quantum dynamics of quasiparticles in gapped graphene. When a cone is formed from a graphene sheet, the topological defect introduced in the system gives rise to some nontrivial holonomies [15, 16, 22]. The boundary conditions associated with the holonomies can be realized by introducing a suitable flux tube, analogous to a cosmic string, passing through the origin [1, 2, 66–70]. In our analysis, such a flux tube shall be used to model the conical topological defect on the 2D graphene sheet. Let us now consider the effect of an external Coulomb charge impurity in such a system, whose strength could be either subcritical or supercritical. For a subcritical Coulomb charge impurity in the presence of the flux tube, we shall show that the quantization of the gapped graphene system is not unique and an additional parameter is required to fully characterize the boundary conditions at the origin. In order to understand the physical meaning of such a boundary condition, recall that the Dirac description in

*Electronic address: baishali.chakraborty@saha.ac.in

†Electronic address: kumars.gupta@saha.ac.in

‡Electronic address: siddhartha.sen@tcd.ie

graphene is valid for low energy or long wavelength excitations. On the other hand, the topological defect as well as the Coulomb charge can lead to additional short range interactions, which cannot be incorporated as dynamical terms in the Dirac equation. The combined effect of the short range interactions due to the topological defect and the Coulomb charge impurity can however be encoded in the boundary conditions[71–74]. If we further impose the natural requirement that the graphene system conserves probability and the time evolution is unitary, then all the allowed boundary conditions can be labelled by a single real parameter. This leads to a one parameter quantization of the gapped graphene system, analogous to what was obtained for Dirac fermions in 2+1 dimensional gravity with a topological defect [1, 2]. For the gapped graphene system, we show that the experimental observables such as the LDOS, phase shifts and the bound state energies depend explicitly on the new parameter that labels the allowed boundary conditions.

For a supercritical value of the charge impurity in the presence of the topological defect, we study the system with a regularized Coulomb potential and also with a zigzag edge boundary condition. The regularization of the Coulomb potential takes care of the finite size of the external charge impurity and allows the bound states of the system to dive into the negative energy continuum[58, 61]. The critical charge in gapped graphene cone is renormalized to a value higher than that of the gapless case and the value depends on the gap, the cut off parameter, the topology of the system and also on the boundary conditions used to obtain the quasibound state spectra in the supercritical region. It will be shown that with the increase in gap or cut off parameter the critical charge in presence of zigzag edge boundary condition increases more rapidly than in presence of a regularized Coulomb potential.

This paper is organized as follows. In the next Section we set up the Dirac equation for gapped graphene cone with a point charge at the apex. This is followed by the analysis of the spectrum in the subcritical region, where we obtain the scattering phase shifts, bound state energies and local density of states (LDOS) and show how these physical quantities depend explicitly on the sample topology. Then we discuss the effect of generalized boundary conditions on the spectrum. In the next section the analysis of the corresponding spectrum is done in the supercritical region with a regularized Coulomb potential and with zigzag edge boundary condition. We end this paper with some discussion and outlook.

II. DIRAC EQUATION FOR A GAPPED GRAPHENE CONE WITH A COULOMB CHARGE

Graphene has a hexagonal honeycomb lattice structure which is formed by two inter penetrating triangular sublattices [4–6, 8, 9] A and B . Assuming only nearest neighbour hopping in graphene and parameterizing the energy difference between the sublattices by ε we have the Hamiltonian as [8]

$$H = \beta \sum_{\vec{R}_A, i} [U_A^\dagger(\vec{R}_A)U_B(\vec{R}_A + \vec{u}_i) + U_B^\dagger(\vec{R}_A + \vec{u}_i)U_A(\vec{R}_A)] + \varepsilon \sum_{\vec{R}_A} [U_A^\dagger(\vec{R}_A)U_A(\vec{R}_A) - U_B^\dagger(\vec{R}_A + \vec{u}_1)U_B(\vec{R}_A + \vec{u}_1)]. \quad (1)$$

Here U_A^\dagger and U_A (U_B^\dagger and U_B) are the creation and destruction operators for electrons localized on sites A (B) respectively. The vectors \vec{u}_i ($i = 1, 2, 3$) connect one A sublattice point to its three neighbouring B sublattice points. The hopping parameter β is related to the probability amplitude for electron transfer between neighbouring sites[6–12]. Though for an ideal single layer graphene $\varepsilon = 0$, by breaking the sublattice symmetry a gap can be introduced in graphene[33–50] and in our following work we shall consider the massive Dirac excitations of a gapped graphene cone.

From the Hamiltonian H we obtain that in gapped graphene the energy eigenvalues are minimum at the six vertices of the first Brillouin zone of graphene and they are known as the Dirac points. Among these points, two are inequivalent [4–6, 8, 9]. We consider them to be situated at the opposite corners of the Brillouin zone and we denote their wave vectors by \mathbf{K}_1 and \mathbf{K}_2 . Thus we can construct the four linearly independent energy eigenstates [6, 9, 10] of the hopping Hamiltonian denoted by $|K_1, A\rangle$, $|K_1, B\rangle$, $|K_2, A\rangle$ and $|K_2, B\rangle$. The pseudospin indices A and B in the eigenstates correspond to that sublattice on which the wavefunction has nonzero amplitude and the valley indices K_1 and K_2 in the eigenstates are distinguished by the manner in which the phase of the wavefunction evolves around a lattice site having zero amplitude wavefunction [24] (see Fig.1). It can also be seen from Fig.1 that the states with valley index K_2 can be produced by rotating the corresponding states with valley index K_1 by 180° [16]. The basis is chosen in such a manner that $\mathbf{K}_2 = -\mathbf{K}_1$. The low energy eigenstates in graphene can be expressed as a linear combination of these energy eigenstates multiplied by envelope functions varying slowly on the lattice parameter scale.

The low-energy properties of the quasiparticle states in graphene near the Dirac point having valley index K_1 , can be described by the Dirac equation

$$H\Psi = [-i(\sigma_1\partial_x + \sigma_2\partial_y) + m\sigma_3]\Psi = E\Psi, \quad (2)$$

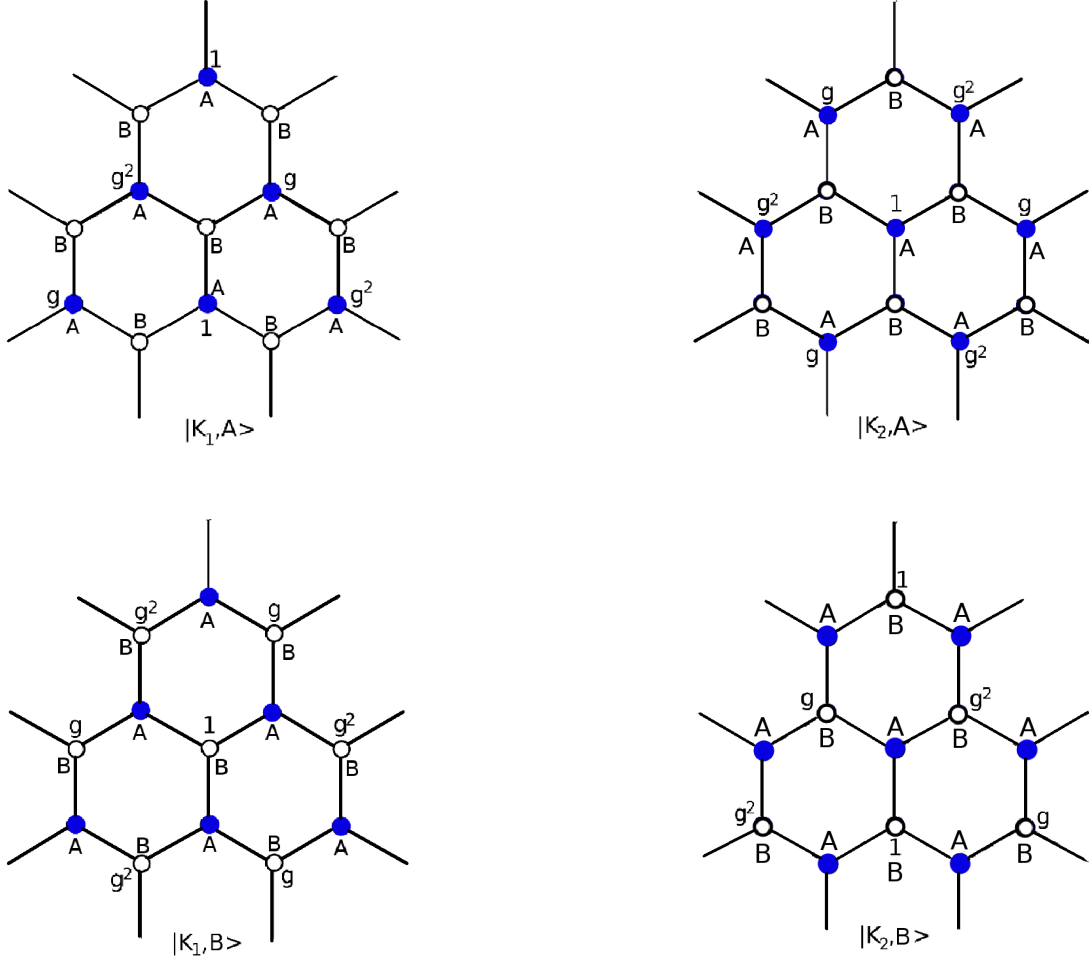


FIG. 1: The linearly independent energy eigenstates of graphene are shown. Here the solid and empty circles belong to sublattice A and B respectively. 1, g and g^2 represent the nonzero amplitudes of the wavefunction at the lattice sites where they are assigned and the wavefunction has zero amplitude at all the other remaining lattice sites. Here $g = \exp(i2\pi/3)$ and $g^2 = \exp(-i2\pi/3)$.

where m denotes the Dirac mass generated due to sublattice symmetry breaking, E is the energy eigenvalue and we have set $\hbar = v_F = 1$. The Hamiltonian acts on the array of the slowly varying envelope functions $\Psi = \begin{pmatrix} \Psi_{K_1,A} \\ \Psi_{K_1,B} \end{pmatrix}$

The Pauli matrices $\sigma_{1,2,3}$ act on the pseudospin indices A, B .

To study the effect of topology on this system, the formation of a graphene cone is considered by introducing local defects in the hexagonal lattice structure of graphene[15, 16]. When a sector is removed from the plane sheet of graphene and the two edges of the sector are identified, the frame $\{\hat{e}_x, \hat{e}_y\}$ becomes discontinuous across the joining line. Therefore we choose a new set of frames $\{\hat{e}_{x'}, \hat{e}_{y'}\}$ which is rotated with respect to the old frame by an angle $\varphi = \theta + \frac{\pi}{2}$ in the counter clockwise direction (see Fig.2). The x' and y' axes are chosen along the \hat{e}_θ direction and the $-\hat{e}_r$ direction respectively [15, 16].

For this change of reference frame the wave function has to be transformed by $\exp(i\varphi\sigma_3/2)$ to keep the form of the Hamiltonian the same[15, 16]. Thus the conical topology gives rise to nontrivial holonomies for the pseudoparticle wavefunctions. When a cone with angle of deficit $\frac{2n\pi}{6}$ is formed, where n can take only discrete values 1, 2, 3, 4, 5, the angular boundary condition obeyed by the Dirac spinor as it goes around a closed path is given by

$$\Psi(r, \theta = 2\pi) = e^{i2\pi(1-\frac{\pi}{6})\frac{\sigma_3}{2}} \Psi(r, \theta = 0). \quad (3)$$

Here (r, θ) denotes the polar coordinate of the lattice points.

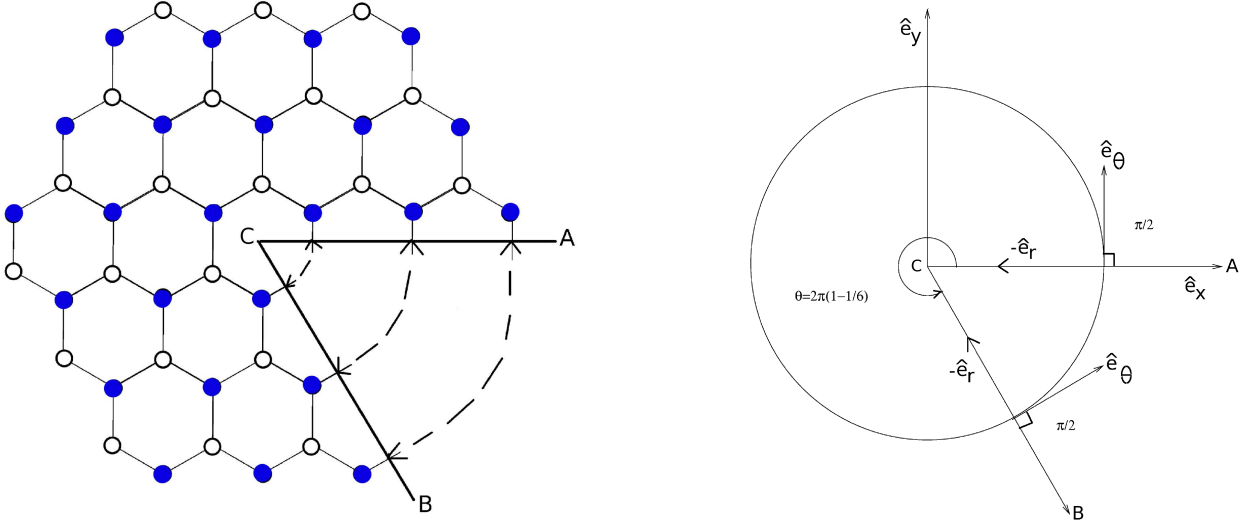


FIG. 2: Formation of cone from plane graphene sheet and rotation of the coordinate system in order to make it continuous.

When the cone is formed by removing odd number of wedges of angle $\frac{2\pi}{6}$ from the plane graphene sheet and the two edges of the removed portion are identified, the adjacent sites on two sides of the identification line belong to the same sublattice (see Fig.2). Thus the bipartite nature of the hexagonal lattice is broken. Also from Fig.1 we can see that rotation of a state with valley index K_1 by an odd multiple of angle $\frac{2\pi}{6}$ gives the corresponding state with valley index K_2 with the same sublattice label. Therefore the removal of odd number of wedges of angle $\frac{2\pi}{6}$ gives rise to an additional phase shift affecting the valley indices of the wave function in the boundary condition[15–17, 24]. The states with valley index K_2 will be affected in the same manner as the states with valley index K_1 but there will be a relative phase difference of 180° between them. Therefore this boundary condition can be described by involving a τ_2 matrix in it where the matrix τ_2 operate on the valley indices[15, 16, 76]. When n is even, this off diagonal matrix does not play any role and the exponential factor appearing in the boundary condition just gives ± 1 depending on the value of n . We diagonalize the matrix τ_2 for all allowed odd values of n . As a result the valley indices of the electronic states become mixtures of K_1 and K_2 . Then the angular boundary condition satisfied for all values of n , by a branch of electronic states having a fixed Fermi index, is given by [15, 16]

$$\Psi(r, \theta = 2\pi) = e^{i2\pi[\pm\frac{n}{4}\sigma_0 + (1-\frac{n}{6})\frac{\sigma_3}{2}]} \Psi(r, \theta = 0). \quad (4)$$

Here σ_0 is an identity matrix which acts on the pseudospin indices A, B . $\Psi = \begin{pmatrix} \Psi_{A,K'} \\ \Psi_{B,K'} \end{pmatrix}$ where K' is a mixture of K_1 and K_2 .

The effect of these holonomies can be modelled by introducing a fictitious magnetic flux tube [19] passing through the apex of the cone. The magnetic vector potential modifies the boundary condition on a Dirac spinor as

$$\Psi(r, \theta = 2\pi) = e^{ie \oint \vec{A} \cdot \vec{dl}} \Psi(r, \theta = 0). \quad (5)$$

Here \vec{dl} is a line element on the circumference of the cone at a distance r from the apex, i.e.

$$\vec{dl} = \hat{e}_\theta r(1 - \frac{n}{6})d\theta. \quad (6)$$

Substituting (6) in (5) and assuming that the component A_θ of the magnetic vector potential is independent of the angle θ , we have from Eq.(4)

$$A_\theta = \frac{1}{er} [\pm \frac{n}{4}\sigma_0 + \frac{\sigma_3}{2}]. \quad (7)$$

Then an external Coulomb charge localized at the apex of the gapped graphene cone can be equivalently described by a suitable combination of electric charge and magnetic flux tube [76]. Let us assume that the Coulomb interaction strength is $\alpha = \frac{Ze^2}{\kappa}$, where Z is the atomic number of the impurity, e is the electronic charge and κ is the dielectric constant. Replacing the ordinary derivatives in the Hamiltonian by the corresponding covariant derivatives, the Dirac equation for the low energy excitations of gapped graphene cone in presence of a Coulomb charge at its apex is given by

$$H\Psi(r, \theta) = \begin{pmatrix} m - \frac{\alpha}{r} & \partial_r - \frac{i}{r(1-\frac{n}{6})}\partial_\theta \pm \frac{\frac{n}{4}}{r(1-\frac{n}{6})} + \frac{1}{2r} \\ -\partial_r - \frac{i}{r(1-\frac{n}{6})}\partial_\theta \pm \frac{\frac{n}{4}}{r(1-\frac{n}{6})} - \frac{1}{2r} & -m - \frac{\alpha}{r} \end{pmatrix} \begin{pmatrix} \Psi_A(r, \theta) \\ \Psi_B(r, \theta) \end{pmatrix} = E \begin{pmatrix} \Psi_A(r, \theta) \\ \Psi_B(r, \theta) \end{pmatrix}. \quad (8)$$

Let

$$\Psi(r, \theta) = \sum_j \begin{pmatrix} \Psi_A^{(j)}(r) \\ \Psi_B^{(j)}(r) \end{pmatrix} e^{ij\theta}, \quad (9)$$

where j is half-integer. Substituting (9) in (8), we obtain that the leading short distance behavior of the wavefunction is given by

$$\Psi_{A,B}^{(j)}(r) \sim r^{\gamma-\frac{1}{2}} \quad \text{where} \quad \gamma = \sqrt{\nu^2 - \alpha^2} \quad \text{and} \quad \nu = \frac{(j \pm \frac{n}{4})}{(1 - \frac{n}{6})}. \quad (10)$$

We should note that the angular part of the wave function is different from that of the planer case, due to the choice of the reference frame[16]. From (10) we can see that when $|\alpha|$ exceeds $|\nu|$, γ becomes imaginary. Therefore, the eigenstates $\Psi_A^{(j)}(r)$ and $\Psi_B^{(j)}(r)$ becomes wildly oscillatory and have no well defined limit as $r \rightarrow 0$. For massive excitations the critical coupling α_c corresponds to that value of α for which $E = -m$. When $m = 0$, the value of α_c is equal to the minimum allowed value of ν and depending on the magnitude of Dirac mass and boundary conditions α_c increases gradually from ν . It will be shown that the critical coupling for the gapped graphene cone explicitly depends on the angle of the cone and also on the product of gap and cutoff parameter. From the expression of ν one can see that if we consider the expression $\nu = \frac{(j - \frac{n}{4})}{(1 - \frac{n}{6})}$ and $j = \frac{3}{2}$, then $\nu = \frac{3}{2}$ for all values of n . Therefore for analyzing the effect of topology the angular momentum channel $j = \frac{3}{2}$ has not been considered.

Depending on the strength of the external Coulomb charge compared to that of the critical charge of a gapped graphene cone with a particular opening angle, the effect of the charge impurity on the cone can be analyzed in two separate regions: subcritical and supercritical.

III. DIRAC EQUATION FOR A GAPPED GRAPHENE CONE WITH A SUBCRITICAL COULOMB CHARGE

In this Section we discuss the bound and scattering state solutions of the Dirac fermions in a gapped graphene cone in the presence of an external Coulomb charge impurity. Following [36], consider the ansatz

$$\Psi_A^j(\rho) = \sqrt{m + E} e^{-\frac{\rho}{2}} \rho^{\gamma-\frac{1}{2}} [F(\rho) + G(\rho)] \quad (11)$$

and

$$\Psi_B^j(\rho) = \sqrt{m - E} e^{-\frac{\rho}{2}} \rho^{\gamma-\frac{1}{2}} [F(\rho) - G(\rho)], \quad (12)$$

where $\rho = 2\eta r$, $\eta = \sqrt{m^2 - E^2}$, $\gamma = \sqrt{\nu^2 - \alpha^2}$, $\nu = \frac{(j \pm \frac{n}{4})}{(1 - \frac{n}{6})}$ and total angular momentum j takes all half integer values. Using Eqs. (8), (9), (11) and (12) we get

$$H_\rho \begin{pmatrix} F(\rho) \\ G(\rho) \end{pmatrix} = \begin{pmatrix} \rho \frac{d}{d\rho} + \left(\gamma - \frac{\alpha E}{\eta}\right) & -\left(\nu + \frac{m\alpha}{\eta}\right) \\ \left(-\nu + \frac{m\alpha}{\eta}\right) & \rho \frac{d}{d\rho} + \left(\gamma - \rho + \frac{\alpha E}{\eta}\right) \end{pmatrix} \begin{pmatrix} F(\rho) \\ G(\rho) \end{pmatrix} = 0, \quad (13)$$

where H_ρ denotes the radial Dirac operator. From Eq.(13) we have

$$\rho \frac{dF}{d\rho} + \left(\gamma - \frac{\alpha E}{\eta}\right) F - \left(\nu + \frac{m\alpha}{\eta}\right) G = 0. \quad (14)$$

and

$$\rho \frac{dG}{d\rho} + \left(\gamma - \rho + \frac{\alpha E}{\eta} \right) G + \left(-\nu + \frac{m\alpha}{\eta} \right) F = 0. \quad (15)$$

Substituting the expression of G from Eq.(14) in Eq.(15) we have

$$\rho F'' + (1 + 2\gamma - \rho)F' - \left(\gamma - \frac{\alpha E}{\eta} \right) F = 0. \quad (16)$$

In order to proceed, for the moment we assume that the wavefunction vanishes at the charge impurity. Solutions of Eq. (16) which obey that boundary condition are given by [75]

$$F(\rho) = A_1 M \left(\gamma - \frac{E\alpha}{\eta}, 1 + 2\gamma, \rho \right), \quad (17)$$

where A_1 is a constant. From Eq.(14) we have

$$G(\rho) = \frac{\left(\gamma - \frac{\alpha E}{\eta} \right)}{\left(\nu + \frac{m\alpha}{\eta} \right)} A_1 M \left(1 + \gamma - \frac{E\alpha}{\eta}, 1 + 2\gamma, \rho \right). \quad (18)$$

The upper and lower components of the wavefunctions are

$$\Psi_A^j(\rho) = A_1 \sqrt{m + E} e^{-\frac{E}{2}\rho} \rho^{\gamma - \frac{1}{2}} \left[M \left(\gamma - \frac{E\alpha}{\eta}, 1 + 2\gamma, \rho \right) + \frac{\left(\gamma - \frac{\alpha E}{\eta} \right)}{\left(\nu + \frac{m\alpha}{\eta} \right)} M \left(1 + \gamma - \frac{E\alpha}{\eta}, 1 + 2\gamma, \rho \right) \right] \quad (19)$$

and

$$\Psi_B^j(\rho) = A_1 \sqrt{m - E} e^{-\frac{E}{2}\rho} \rho^{\gamma - \frac{1}{2}} \left[M \left(\gamma - \frac{E\alpha}{\eta}, 1 + 2\gamma, \rho \right) - \frac{\left(\gamma - \frac{\alpha E}{\eta} \right)}{\left(\nu + \frac{m\alpha}{\eta} \right)} M \left(1 + \gamma - \frac{E\alpha}{\eta}, 1 + 2\gamma, \rho \right) \right]. \quad (20)$$

Bound states occur when the wavefunctions reduce to polynomials i.e. when

$$\gamma - \frac{\alpha E}{\eta} = -p, \quad (21)$$

where

$$p = \begin{cases} 0, 1, 2, \dots, & \text{when } \nu > 0, \\ 1, 2, 3, \dots, & \text{when } \nu < 0. \end{cases} \quad (22)$$

The corresponding bound state spectra is obtained as

$$E_p = \frac{m \operatorname{sgn}(\alpha)}{\sqrt{1 + \frac{\alpha^2}{(p+\gamma)^2}}}. \quad (23)$$

Here the energy should be of the same sign (positive or negative) as α because otherwise the value of p will become negative and in our range of interest, it is not allowed.

The solution of Eq.(13) which leads to physical scattering states when $|E| > |m|$ is [75]

$$F(\rho) = A_1 M \left(\gamma - \frac{E\alpha}{\eta}, 1 + 2\gamma, \rho \right) + A_2 \rho^{-2\gamma} M \left(-\gamma - \frac{E\alpha}{\eta}, 1 - 2\gamma, \rho \right). \quad (24)$$

From Eq.(14) we have

$$G(\rho) = \frac{\left(\gamma - \frac{\alpha E}{\eta} \right)}{\left(\nu + \frac{m\alpha}{\eta} \right)} A_1 M \left(1 + \gamma - \frac{E\alpha}{\eta}, 1 + 2\gamma, \rho \right) - \frac{\left(\gamma + \frac{\alpha E}{\eta} \right)}{\left(\nu + \frac{m\alpha}{\eta} \right)} A_2 \rho^{-2\gamma} M \left(1 - \gamma - \frac{E\alpha}{\eta}, 1 - 2\gamma, \rho \right). \quad (25)$$

Here the parameter $\eta = \sqrt{m^2 - E^2}$ is purely imaginary, i.e. $\eta = -ik$, [36] where k is defined as $k = \sqrt{E^2 - m^2}$. Consequently, the variable ρ also becomes purely imaginary, $\rho = -2ikr$. Using the $r \rightarrow \infty$ limit of the scattering states the scattering matrix is obtained as

$$S(k) = (2ik)^{\frac{2i\alpha E}{k}} \frac{(\nu + i\frac{m\alpha}{k}) \Gamma(1 + \gamma - i\frac{\alpha E}{k})}{(\gamma - i\frac{E\alpha}{k}) \Gamma(1 + \gamma + i\frac{E\alpha}{k})} e^{i\pi(\gamma + i\frac{\alpha E}{k})}. \quad (26)$$

From Eq.(26) it can be seen that the poles of the S matrix determined by $(1 + \gamma - i\frac{\alpha E}{k}) = 1 - p$, where p is a nonzero positive integer and $(\gamma - i\frac{E\alpha}{k}) = 0$ when $\nu > 0$, gives back the corresponding bound states as expected.

A. Generalized boundary conditions

The Dirac equation discussed in the previous section is valid for low energy or long wavelength excitations. The conical defect as well as the Coulomb charge impurity might give rise to short range interactions in the system, which cannot be incorporated as dynamical terms in the Dirac equation. However, the combined effect of those short range interactions can be taken into account through the choice of suitable boundary conditions. In systems with unitary time evolution, there is a well defined prescription due to von Neumann to determine the allowed boundary conditions, which is what we shall follow [71–74].

From Eq.(8) it can be seen that the Dirac operator H has an angular part and a radial part. The angular part operates on a domain $Y(\theta)$ which is spanned by the antiperiodic functions $e^{ij\theta}$ where j is a half integer and the corresponding boundary condition is kept unchanged. The radial Dirac operator H_ρ , given by Eq.(13), is symmetric in the domain $\mathcal{D}_0 = C_0^\infty(R^+)$ which consists of infinitely differentiable functions of compact support in the real half line R^+ and its adjoint operator H_ρ^\dagger has the same expression as H_ρ but its domain can be different. Now to determine the domain of self-adjointness of the Dirac operator H , consider the equations

$$H^\dagger \Psi_\pm = \pm \frac{i}{d} \Psi_\pm, \quad (27)$$

where d has the dimension of length. The total number of square integrable, linearly independent solutions of Eq.(27) gives the deficiency indices for H and they are denoted by n_\pm . For obtaining n_\pm , Eq.(13) is considered with E replaced by $\pm \frac{i}{d}$. To understand the significance of these indices we should note that if an operator is self-adjoint, then it is expected to have only real eigenvalues. Thus the existence of imaginary eigenvalues $\pm \frac{i}{d}$ in the spectrum is a measure of the deviation of an operator from self-adjointness. The non zero deficiency indices serve as the measurement of this deviation. Depending on the deficiency indices H_ρ can be classified in three different ways [71] : (1) When $n_+ = n_- = 0$, H_ρ is essentially self-adjoint in $\mathcal{D}_0(H_\rho)$. (2) When $n_+ = n_- \neq 0$, H_ρ is not self-adjoint in $\mathcal{D}_0(H_\rho)$ but it can admit self-adjoint extensions. (3) When $n_+ \neq n_-$, H_ρ cannot have self-adjoint extensions.

To find the deficiency indices n_\pm let us first consider the following.

$$\Psi_{A\pm}^j(\rho) = \sqrt{m \pm \frac{i}{d}} e^{-\frac{\rho}{2}} \rho^{\gamma - \frac{1}{2}} [F_\pm(\rho) + G_\pm(\rho)] \quad (28)$$

and

$$\Psi_{B\pm}^j(\rho) = \sqrt{m \mp \frac{i}{d}} e^{-\frac{\rho}{2}} \rho^{\gamma - \frac{1}{2}} [F_\pm(\rho) - G_\pm(\rho)], \quad (29)$$

where $\rho = 2\eta_1 r$, $\eta_1 = \sqrt{m^2 + \frac{1}{d^2}}$, $\gamma = \sqrt{\nu^2 - \alpha^2}$ and $\nu = \frac{(j \pm \frac{1}{2})}{(1 - \frac{\alpha}{d})}$. Then we can write

$$H_\rho \begin{pmatrix} F_\pm(\rho) \\ G_\pm(\rho) \end{pmatrix} = \begin{pmatrix} \rho \frac{d}{d\rho} + \left(\gamma \mp \frac{i\alpha}{\eta_1 d} \right) & - \left(\nu + \frac{m\alpha}{\eta_1} \right) \\ \left(-\nu + \frac{m\alpha}{\eta_1} \right) & \rho \frac{d}{d\rho} + \left(\gamma - \rho \pm \frac{i\alpha}{\eta_1 d} \right) \end{pmatrix} \begin{pmatrix} F_\pm(\rho) \\ G_\pm(\rho) \end{pmatrix} = 0. \quad (30)$$

From Eq.(30) we have

$$\rho \frac{dF_\pm(\rho)}{d\rho} + \left(\gamma \mp \frac{i\alpha}{\eta_1 d} \right) F_\pm(\rho) - \left(\nu + \frac{m\alpha}{\eta_1} \right) G_\pm(\rho) = 0, \quad (31)$$

and

$$\rho \frac{dG_{\pm}(\rho)}{d\rho} + \left(\gamma - \rho \pm \frac{i\alpha}{\eta_1 d} \right) G_{\pm}(\rho) + \left(-\nu + \frac{m\alpha}{\eta_1} \right) F_{\pm}(\rho) = 0. \quad (32)$$

Substituting the expression of $G_{\pm}(\rho)$ from Eq.(31) in Eq.(32) we have

$$\rho F_{\pm}''(\rho) + (1 + 2\gamma - \rho) F_{\pm}'(\rho) - \left(\gamma \mp \frac{i\alpha}{\eta_1 d} \right) F_{\pm}(\rho) = 0. \quad (33)$$

We first determine the deficiency subspace characterized by $F_+(\rho)$ and $G_+(\rho)$ given in Eq.(30). The required solution of Eq.(33) is

$$F_+(\rho) = U \left(\gamma - \frac{i\alpha}{\eta_1 d}, 1 + 2\gamma, \rho \right). \quad (34)$$

Using the differential recursive relation $zU'(a, b, z) + aU(a, b, z) = a(1 + a - b)U(a + 1, b, z)$, from Eq.(31) we have

$$G_+(\rho) = \frac{\left(\gamma - \frac{i\alpha}{\eta_1 d} \right) \left(-\gamma - \frac{i\alpha}{\eta_1 d} \right)}{\left(\nu + \frac{m\alpha}{\eta_1} \right)} U \left(1 + \gamma - \frac{i\alpha}{\eta_1 d}, 1 + 2\gamma, \rho \right). \quad (35)$$

In the limit $\rho \rightarrow 0$ the functions behave as

$$F_+ \rightarrow \frac{\pi}{\sin \pi(1 + 2\gamma)} (P_+ - Q_+ \rho^{-2\gamma}), \quad (36)$$

$$G_+ \rightarrow \frac{\pi}{\sin \pi(1 + 2\gamma)} (R_+ - S_+ \rho^{-2\gamma}), \quad (37)$$

where

$$P_+ = \frac{1}{\Gamma(-\gamma - \frac{i\alpha}{\eta_1 d}) \Gamma(1 + 2\gamma)} \quad (38)$$

$$Q_+ = \frac{1}{\Gamma(\gamma - \frac{i\alpha}{\eta_1 d}) \Gamma(1 - 2\gamma)} \quad (39)$$

$$R_+ = \frac{\left(\gamma - \frac{i\alpha}{\eta_1 d} \right) \left(-\gamma - \frac{i\alpha}{\eta_1 d} \right)}{\left(\nu + \frac{m\alpha}{\eta_1} \right)} \frac{1}{\Gamma(1 - \gamma - \frac{i\alpha}{\eta_1 d}) \Gamma(1 + 2\gamma)} \quad (40)$$

$$S_+ = \frac{\left(\gamma - \frac{i\alpha}{\eta_1 d} \right) \left(-\gamma - \frac{i\alpha}{\eta_1 d} \right)}{\left(\nu + \frac{m\alpha}{\eta_1} \right)} \frac{1}{\Gamma(1 + \gamma - \frac{i\alpha}{\eta_1 d}) \Gamma(1 - 2\gamma)} \quad (41)$$

are constants depending on the system parameters. From the above relations we find that as $\rho \rightarrow 0$,

$$\int |\psi_{A+}|^2 \rho d\rho \rightarrow \int (a_1 \rho^{2\gamma} + a_2 + a_3 \rho^{-2\gamma}) d\rho, \quad (42)$$

$$\int |\psi_{B+}|^2 \rho d\rho \rightarrow \int (b_1 \rho^{2\gamma} + b_2 + b_3 \rho^{-2\gamma}) d\rho, \quad (43)$$

where a_i, b_i ($i = 1, 2, 3$) are constants, whose explicit forms are not relevant. As γ is a real positive quantity in the subcritical region, from Eq.(42) and (43) it can be shown that ψ_{A+} and ψ_{B+} are square integrable everywhere provided $0 < \gamma < \frac{1}{2}$. Thus $n_+ = 1$ for the parameter range $0 < \gamma < \frac{1}{2}$.

In a similar way, by analyzing the deficiency subspace characterized by the negative sign, we obtain

$$F_- = U \left(\gamma + \frac{i\alpha}{\eta_1 d}, 1 + 2\gamma, \rho \right), \quad (44)$$

$$G_- = \frac{\left(\gamma + \frac{i\alpha}{\eta_1 d} \right) \left(-\gamma + \frac{i\alpha}{\eta_1 d} \right)}{\left(\nu + \frac{m\alpha}{\eta_1} \right)} U \left(1 + \gamma + \frac{i\alpha}{\eta_1 d}, 1 + 2\gamma, \rho \right). \quad (45)$$

In addition, in the limit $\rho \rightarrow 0$ the functions F_- and G_- behave as

$$F_- \rightarrow \frac{\pi}{\sin \pi(1+2\gamma)}(P_- - Q_- \rho^{-2\gamma}), \quad (46)$$

$$G_- \rightarrow \frac{\pi}{\sin \pi(1+2\gamma)}(R_- - S_- \rho^{-2\gamma}), \quad (47)$$

where

$$P_- = \bar{P}_+, \quad Q_- = \bar{Q}_+, \quad R_- = \bar{R}_+, \quad S_- = \bar{S}_+. \quad (48)$$

Similar analysis as before shows that $n_- = 1$ for the parameter range $0 < \gamma < \frac{1}{2}$ as well. Thus for the gapped graphene cone with a charge impurity, $n_+ = n_- = 1$ when $0 < \gamma < \frac{1}{2}$. Therefore, this system admits a one parameter family of self-adjoint extensions for $0 < \gamma < \frac{1}{2}$. We would now like to find out the spectrum of the system in a range of ν and the effective subcritical Coulomb potential strength α such that $0 < \gamma < \frac{1}{2}$. The deficiency subspaces for the radial Dirac operator H_ρ are spanned by the elements,

$$\Psi_\pm = \begin{pmatrix} \Psi_{A\pm} \\ \Psi_{B\pm} \end{pmatrix} = \begin{pmatrix} \sqrt{m \pm \frac{i}{d}} e^{-\frac{\ell}{2}\rho} \rho^{\gamma-\frac{1}{2}} (F_\pm + G_\pm) \\ \sqrt{m \mp \frac{i}{d}} e^{-\frac{\ell}{2}\rho} \rho^{\gamma-\frac{1}{2}} (F_\pm - G_\pm) \end{pmatrix}. \quad (49)$$

The domain in which the Dirac operator is self-adjoint is given by $\mathcal{D}_z(H_\rho) = \mathcal{D}_0(H_\rho) \oplus \{C(e^{i\frac{z}{2}}\Psi_+ + e^{-i\frac{z}{2}}\Psi_-)\}$, where C is an arbitrary complex number and $z \in R \bmod 2\pi$. Thus we have a one parameter family of self-adjoint extensions, labeled by a real parameter z . For each choice of the parameter z , we have a domain of self-adjointness of the radial Dirac operator defined by $\mathcal{D}_z(H_\rho)$. When $\rho \rightarrow 0$ an arbitrary element $\Psi_z \in \mathcal{D}_z(H_\rho)$ can be written as

$$\Psi_z = \begin{pmatrix} \Psi_{Az} \\ \Psi_{Bz} \end{pmatrix} \rightarrow C \begin{pmatrix} \sqrt{m + \frac{i}{d}} e^{\frac{iz}{2}} \rho^{\gamma-\frac{1}{2}} (F_+ + G_+) + \sqrt{m - \frac{i}{d}} e^{-\frac{iz}{2}} \rho^{\gamma-\frac{1}{2}} (F_- + G_-) \\ \sqrt{m - \frac{i}{d}} e^{\frac{iz}{2}} \rho^{\gamma-\frac{1}{2}} (F_+ - G_+) + \sqrt{m + \frac{i}{d}} e^{-\frac{iz}{2}} \rho^{\gamma-\frac{1}{2}} (F_- - G_-) \end{pmatrix}, \quad (50)$$

where F_- and G_- denote the complex conjugates of F_+ and G_+ respectively.

Now the spectrum of the system is found out when the boundary conditions are governed by the domain $\mathcal{D}_z(H_\rho)$. A solution of the physical eigenvalue problem is written as

$$\Psi = N \begin{pmatrix} \sqrt{m + E} e^{-\frac{\ell}{2}\rho} \rho^{\gamma-\frac{1}{2}} (F(\rho) + G(\rho)) \\ \sqrt{m - E} e^{-\frac{\ell}{2}\rho} \rho^{\gamma-\frac{1}{2}} (F(\rho) - G(\rho)) \end{pmatrix} \quad (51)$$

Here F and G satisfy Eqs. (14) and (15) respectively, and N denotes the normalization. Solutions of Eqs.(14) and (15) that are square integrable at infinity are given by

$$F = U \left(\gamma - \frac{\alpha E}{\eta}, 1 + 2\gamma, \rho \right), \quad (52)$$

$$G = U \left(1 + \gamma - \frac{\alpha E}{\eta}, 1 + 2\gamma, \rho \right). \quad (53)$$

Now using Eqs.(50) and (51) we have in the limit $\rho \rightarrow 0$,

$$F \rightarrow \frac{\pi}{\sin \pi(1+2\gamma)}(P - Q \rho^{-2\gamma}), \quad (54)$$

$$G \rightarrow \frac{\pi}{\sin \pi(1+2\gamma)}(R - S \rho^{-2\gamma}), \quad (55)$$

where

$$P = \frac{1}{\Gamma \left(-\gamma - \frac{\alpha E}{\eta} \right) \Gamma(1+2\gamma)} \quad Q = \frac{1}{\Gamma \left(\gamma - \frac{\alpha E}{\eta} \right) \Gamma(1-2\gamma)} \quad (56)$$

$$R = \frac{1}{\Gamma \left(1 - \gamma - \frac{\alpha E}{\eta} \right) \Gamma(1+2\gamma)} \quad S = \frac{1}{\Gamma \left(1 + \gamma - \frac{\alpha E}{\eta} \right) \Gamma(1-2\gamma)}. \quad (57)$$

Hence, as $\rho \rightarrow 0$,

$$\Psi \rightarrow \frac{\pi}{\sin \pi(1+2\gamma)} N \left(\frac{\sqrt{m+E}[(P+R)\rho^{\gamma-(\frac{1}{2})} - (Q+S)\rho^{-\gamma-(\frac{1}{2})}]}{\sqrt{m-E}[(P-R)\rho^{\gamma-(\frac{1}{2})} - (Q-S)\rho^{-\gamma-(\frac{1}{2})}]} \right) \quad (58)$$

The physical solution Ψ in Eq.(58) must belong to the domain of self-adjointness given by $\mathcal{D}_z(H_\rho)$. In fact behavior of the elements of the domain $\mathcal{D}_z(H_\rho)$ determines the boundary conditions for the system. If $\Psi_z \in \mathcal{D}_z(H_\rho)$, then as $\rho \rightarrow 0$ the coefficients of $r^{\gamma-(1/2)}$ and $r^{-\gamma-(1/2)}$ in Eqs. (50) and (58) must match. Let us define

$$\sqrt{m + \frac{i}{d}}(P_+ + R_+) = \chi_1 e^{i\phi_1}$$

$$\text{and } \sqrt{m + \frac{i}{d}}(Q_+ + S_+) = \chi_2 e^{i\phi_2}.$$

Now comparing the terms of Eqs. (50) and (58) we obtain

$$\left(\frac{\eta^2}{\frac{1}{d^2} + m^2} \right)^\gamma \frac{P+R}{Q+S} = \frac{\chi_1 \cos(\phi_1 + \frac{z}{2})}{\chi_2 \cos(\phi_2 + \frac{z}{2})} \quad (59)$$

Using the expressions of the constants P, Q, R and S and the above equation we finally get

$$\begin{aligned} f(E) &\equiv \left(\frac{\eta^2}{\frac{1}{d^2} + m^2} \right)^\gamma \frac{\left(1 - \gamma - \frac{\alpha E}{\eta}\right) \Gamma\left(1 + \gamma - \frac{\alpha E}{\eta}\right) \Gamma(1 - 2\gamma)}{\left(1 + \gamma - \frac{\alpha E}{\eta}\right) \Gamma\left(1 - \gamma - \frac{\alpha E}{\eta}\right) \Gamma(1 + 2\gamma)} \\ &= \frac{\chi_1 \cos(\phi_1 + \frac{z}{2})}{\chi_2 \cos(\phi_2 + \frac{z}{2})}. \end{aligned} \quad (60)$$

Eq.(60) determines the spectrum in terms of the system parameters and the self-adjoint extension parameter z . Each choice of z corresponds to a different boundary condition described by the domain $\mathcal{D}_z(H_\rho)$ and leads to an inequivalent quantum theory. However the choice of z for a particular system is determined empirically as the theory cannot predict its value. For a special choice of $z = z_1$ such that $\phi_2 + \frac{z_1}{2} = \frac{\pi}{2}$, we have

$$\gamma - \frac{E\alpha}{\eta} = -p, \quad p = 1, 2, 3, \dots \quad (61)$$

This leads to the spectrum obtained in Eq.(21) for $0 < \gamma < \frac{1}{2}$. For another special choice of $z = z_2$ such that $\phi_1 + \frac{z_2}{2} = \frac{\pi}{2}$, we get

$$-\gamma - \frac{E\alpha}{\eta} = -p, \quad p = 1, 2, 3, \dots \quad (62)$$

Though Eq.(60) cannot be solved analytically, from a typical plot of $f(E)$ it can be obtained numerically. From Figure (3a) we can see when z changes from -0.8 to 4 , the bound state energy changes from 0.915 to 0.92 . Again when z changes from 4 to 0.1 , the bound state energy changes from 0.92 to 0.942 . Now calculating the contribution to LDOS coming from a single angular momentum channel $j = \frac{3}{2}$ for these three different values of bound state energy, we observe in diagram 3(b) how the r dependence of LDOS varies with different values of z . In Figure (3c) we have shown how the bound state energy depends on the topology of the system for a particular angular momentum channel $j = \frac{1}{2}$ and three self-adjoint extension parameters $z = -0.8, 4$ and 0.1 . From the Figure (3c) we can see when n changes from 3 to 1 , for the self-adjoint extension parameter $z = 0.1$ the bound state energy changes from 0.9935 to 0.9955 . Calculating the contribution to LDOS coming from a single angular momentum channel $j = \frac{1}{2}$ for these two different values of bound state energy, we observe in diagram 3(d) how the topology of a system affects the r dependence of LDOS.

In the scattering state sector where $|E| > |m|$ and $\eta = -ik$ the general solution of Eqs.(14) and (15) that lead to physical scattering states are given by

$$F(\rho) = P_1(k)M\left(\gamma - \frac{E\alpha}{\eta}, 1 + 2\gamma, \rho\right) + Q_1(k)\rho^{-2\gamma}M\left(-\gamma - \frac{E\alpha}{\eta}, 1 - 2\gamma, \rho\right). \quad (63)$$

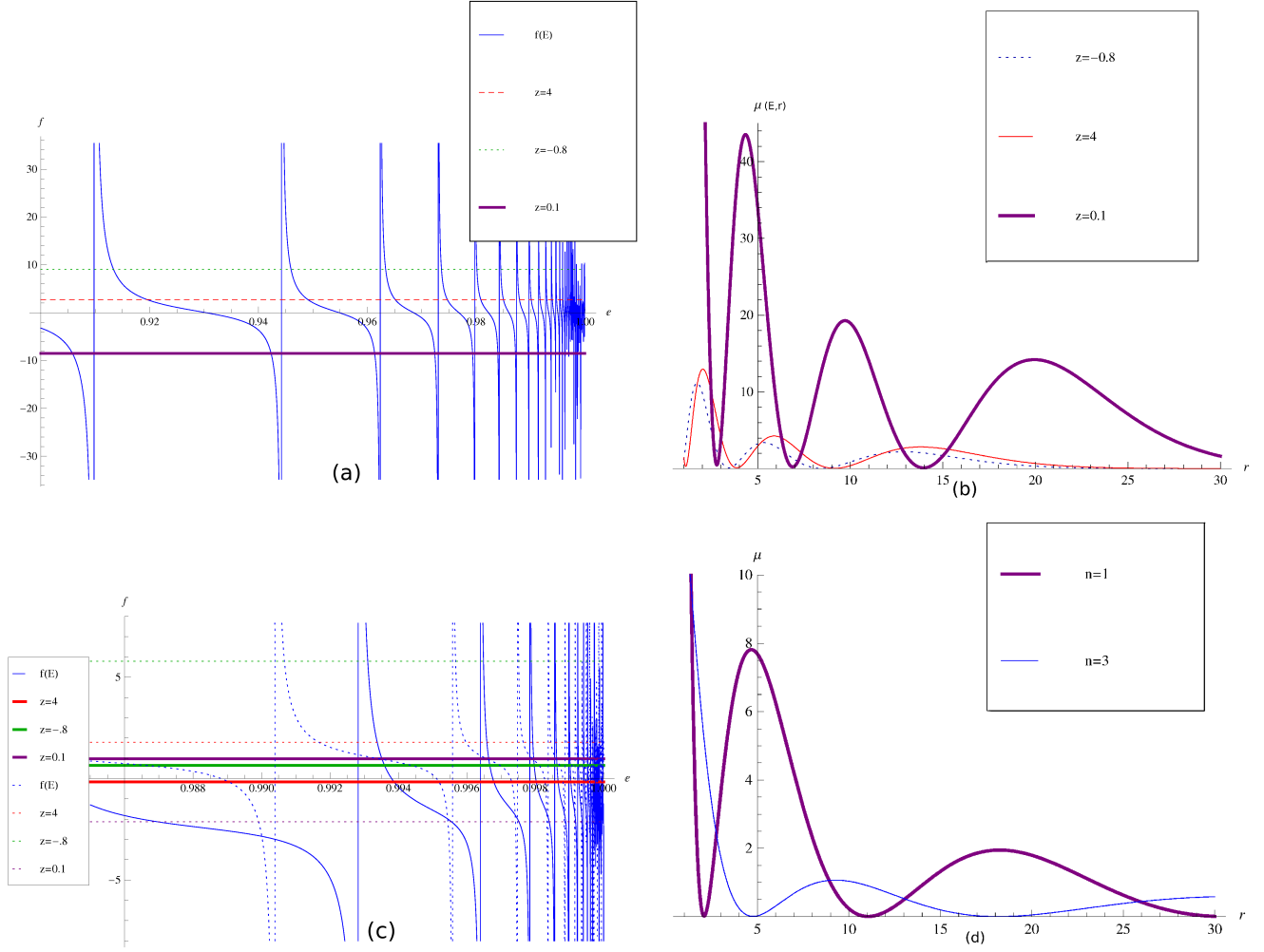


FIG. 3: (a) Plot of $f(E)$ is shown for system parameters $j = \frac{3}{2}$, $n = 1$, $\alpha = 1.48$ and $m = 1$. The three horizontal line corresponds to the three different values of the self adjoint extension parameter $z = 4, 0.1, -0.8$. (b) Dependence of LDOS in the bound state sector of the gapped graphene cone on the distance r from the external charge impurity is shown for three different values of bound state energy corresponding to three different values of self adjoint extension parameter. Here the contribution from angular momentum channel $j = \frac{3}{2}$ is shown and the system parameters are $n = 1$, $\alpha = 1.48$ and $m = 1$. We have assumed $d=1$. (c) Plot of $f(E)$ is shown for two different values of n (1 and 3) with system parameters $j = \frac{1}{2}$, $\alpha = 0.29$ and $m = 1$. The three horizontal line corresponds to the three different values of the self adjoint extension parameter $z = 4, 0.1, -0.8$. The solid lines correspond to $n = 3$ and the dotted lines correspond to $n = 1$. (d) Dependence of LDOS on the distance r from the external charge impurity is shown for two different values of bound state energy corresponding to two different values of n with the self-adjoint extension parameter $z = 0.1$. Here the contribution from angular momentum channel $j = \frac{1}{2}$ is shown and the system parameters are $\alpha = 0.29$ and $m = 1$.

From Eq.(14) we have

$$G(\rho) = \frac{\left(\gamma - \frac{\alpha E}{\eta}\right)}{\left(\nu + \frac{m\alpha}{\eta}\right)} P_1(k) M\left(1 + \gamma - \frac{E\alpha}{\eta}, 1 + 2\gamma, \rho\right) - \frac{\left(\gamma + \frac{\alpha E}{\eta}\right)}{\left(\nu + \frac{m\alpha}{\eta}\right)} Q_1(k) \rho^{-2\gamma} M\left(1 - \gamma - \frac{E\alpha}{\eta}, 1 - 2\gamma, \rho\right). \quad (64)$$

Substituting these expressions of F and G in Eq (11) and Eq (12) we get the upper and lower components of the wave function. Then from the asymptotic form of the wavefunction, identifying the incoming and outgoing waves, the scattering matrix and the phase shifts are obtained. Now, to find a relation between the constants $P_1(k)$ and $Q_1(k)$, we consider the short distance limit of the wave function. The domain of self-adjointness of the Hamiltonian H_ρ is given by $\mathcal{D}_z(H_\rho) = \mathcal{D}(H_\rho) \oplus \{e^{i\frac{z}{2}}\Psi_+ + e^{-i\frac{z}{2}}\Psi_-\}$. In the limit $r \rightarrow 0$, an element of the domain $\mathcal{D}_z(H_\rho)$ can be given

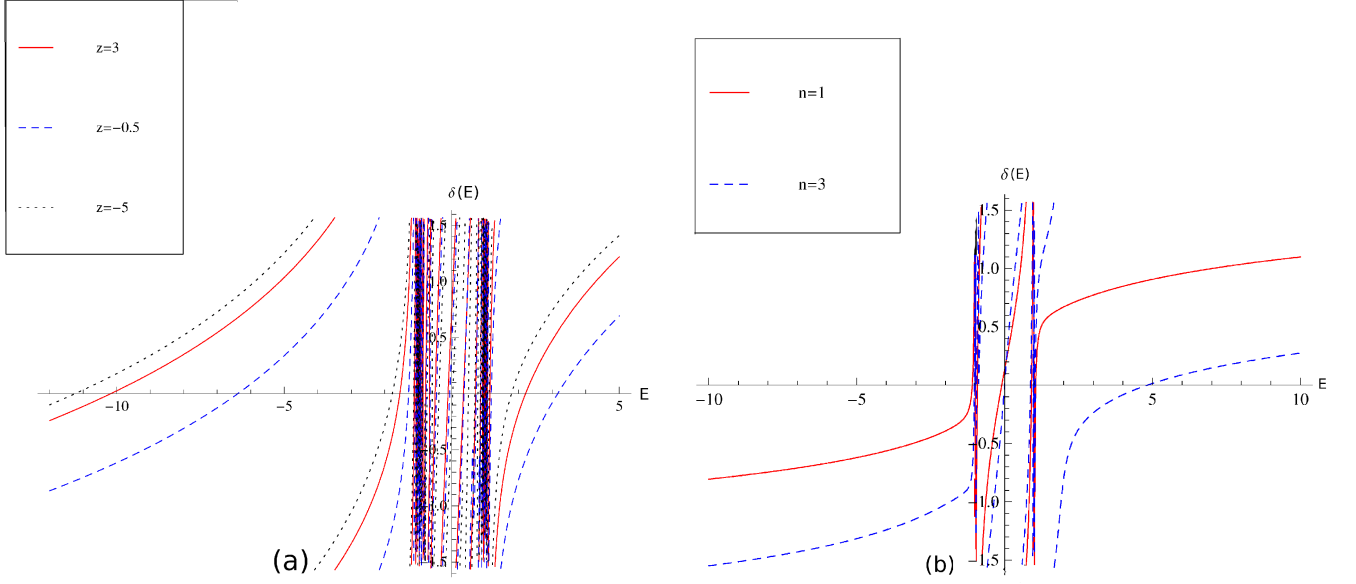


FIG. 4: (a) Phase shifts in the gapped graphene cone is shown for three different values of the self adjoint extension parameter $z = 3, -0.5, -5$ where the system parameters are $n = 1, j = \frac{3}{2}, \alpha = 1.48$, and $m = 1$. (b) Scattering phase shifts are shown for different angles of the gapped graphene cone with the sae parameter $z = -0.5$ and system parameters $j = \frac{1}{2}, \alpha = 0.29$ and $m = 1$.

by

$$\Psi = C \left(e^{i\frac{z}{2}} \Psi_+ + e^{-i\frac{z}{2}} \Psi_- \right), \quad (65)$$

where C is an arbitrary constant.

After using the relation (65) and matching the coefficients of appropriate powers of r at both sides in (65), we get the following two conditions

$$\begin{aligned} & (2\eta)^{\gamma-\frac{1}{2}} \left(1 + \frac{\gamma - \frac{\alpha E}{\eta}}{\nu + \frac{m\alpha}{\eta}} \right) P_1(k) \sqrt{m+E} \\ &= C \frac{\pi}{\sin \pi(1+2\gamma)} \left(\sqrt{m + \frac{i}{d}} e^{i\frac{z}{2}} (P_+ + R_+) + \sqrt{m - \frac{i}{d}} e^{-i\frac{z}{2}} (\bar{P}_+ + \bar{R}_+) \right) (2\eta_1)^{\gamma-\frac{1}{2}} \end{aligned} \quad (66)$$

and

$$\begin{aligned} & (2\eta)^{-\gamma-\frac{1}{2}} \left(1 - \frac{\gamma + \frac{\alpha E}{\eta}}{\nu + \frac{m\alpha}{\eta}} \right) Q_1(k) \sqrt{m+E} \\ &= -C \frac{\pi}{\sin \pi(1+2\gamma)} \left(\sqrt{m + \frac{i}{d}} e^{i\frac{z}{2}} (Q_+ + S_+) + \sqrt{m - \frac{i}{d}} e^{-i\frac{z}{2}} (\bar{Q}_+ + \bar{S}_+) \right) (2\eta_1)^{-\gamma-\frac{1}{2}}, \end{aligned} \quad (67)$$

where z is the self-adjoint extension parameter. The equations Eq.(66) and Eq.(67) yield

$$\frac{(\nu + \frac{m\alpha}{\eta} + \gamma - \frac{\alpha E}{\eta}) P_1(k)}{(\nu + \frac{m\alpha}{\eta} - \gamma - \frac{\alpha E}{\eta}) Q_1(k)} = - \frac{\sqrt{m + \frac{i}{d}} e^{i\frac{z}{2}} (P_+ + R_+) + \sqrt{m - \frac{i}{d}} e^{-i\frac{z}{2}} (\bar{P}_+ + \bar{R}_+)}{\sqrt{m + \frac{i}{d}} e^{i\frac{z}{2}} (Q_+ + S_+) + \sqrt{m - \frac{i}{d}} e^{-i\frac{z}{2}} (\bar{Q}_+ + \bar{S}_+)} (2\eta_1)^{2\gamma} (2\eta)^{-2\gamma}$$

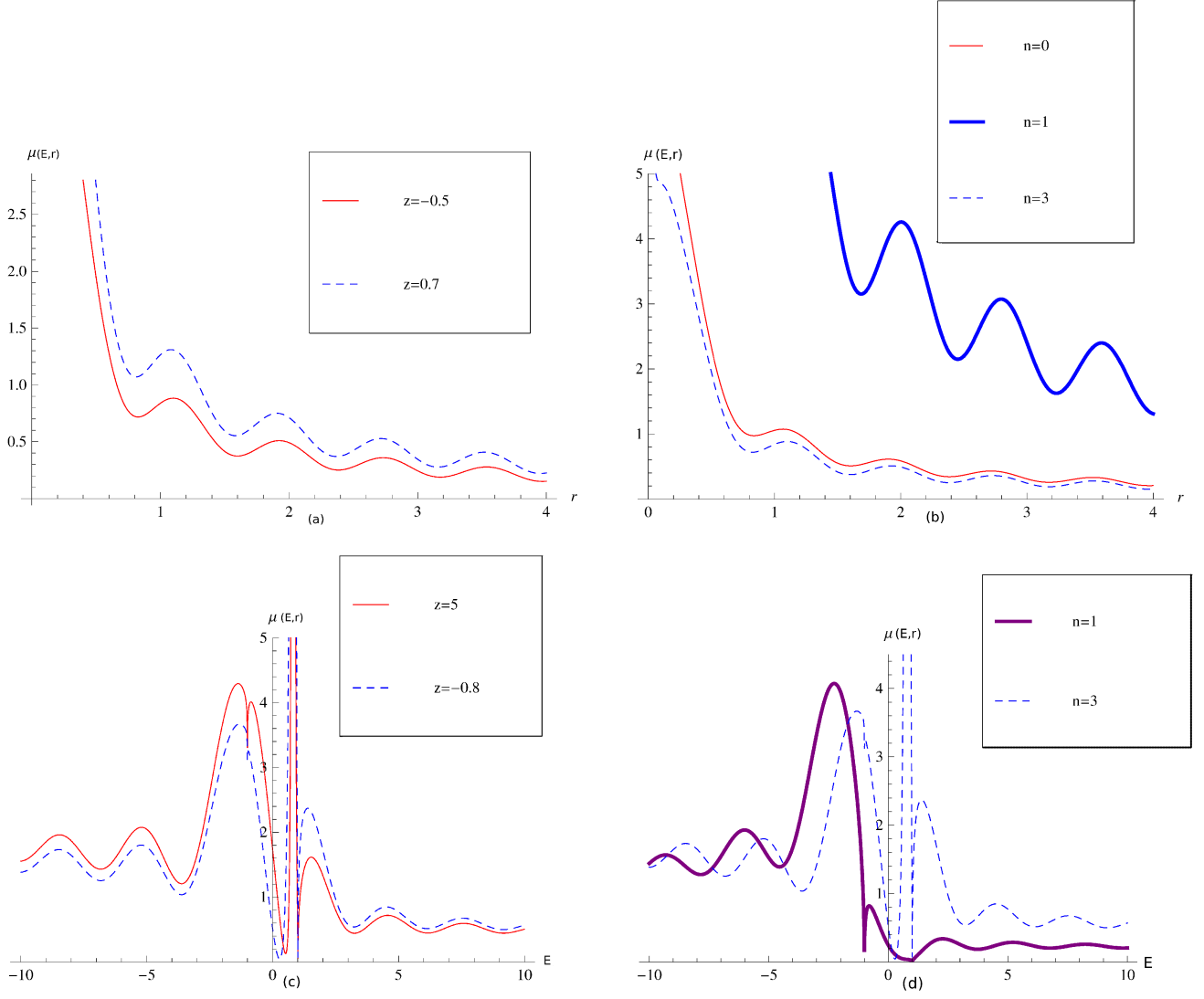


FIG. 5: (a) Dependence of LDOS on the distance r from the Coulomb impurity is shown for two different values of sae parameter $z = -0.5, 0.7$ and a particular value of $E = 4$ and with $j = \frac{1}{2}$, $n = 3$, $\alpha = 0.29$ and $m = 1$. (b) Effect of topology on r dependence of LDOS is shown for sae parameter $z = -0.5$, $E = 4$ and system parameters $\alpha = 0.29$, $n = 1, 3$ and $m = 1$ considering contribution coming from the angular momentum channel $j = \frac{1}{2}$. (c) Energy dependence of LDOS is shown for two different values of sae parameter $z = 5, -0.8$ at a distance $r = 1$ from the external Coulomb impurity. The system parameters used for the plot are $\alpha = 0.29$ and $m = 1$ and contribution coming from the angular momentum channel $j = \frac{1}{2}$ is considered. (d) Effect of topology on the energy dependence of LDOS is shown for sae parameter $z = -0.8$, angular momentum channel $j = \frac{1}{2}$ and system parameters $\alpha = -0.29$, $n = 1, 3$ and $m = 1$

$$= -\frac{\chi_1 \cos(\phi_1 + \frac{z}{2})}{\chi_2 \cos(\phi_2 + \frac{z}{2})} (2\eta_1)^{2\gamma} (2\eta)^{-2\gamma}, \quad (68)$$

where we have defined $\sqrt{m + \frac{i}{d}(P_+ + R_+)} \equiv \chi_1 e^{i\phi_1}$ and $\sqrt{m + \frac{i}{d}(Q_+ + S_+)} \equiv \chi_2 e^{i\phi_2}$. Using the relations between the constants given before and (68), the scattering matrix can now be written as

$$\mathbf{S}(k) = (2ik)^{2i\frac{\alpha E}{k}} \frac{-\frac{\chi_1 \cos(\phi_1 + \frac{z}{2})}{\chi_2 \cos(\phi_2 + \frac{z}{2})} (2\eta_1)^{2\gamma} (2\eta)^{-2\gamma} \frac{1+f_2}{1+f_1} f_1 \frac{\Gamma(1+2\gamma)}{\Gamma(1+\gamma+i\frac{\alpha E}{k})} + f_2 \frac{\Gamma(1-2\gamma)}{\Gamma(1-\gamma+i\frac{\alpha E}{k})}}{-\frac{\chi_1 \cos(\phi_1 + \frac{z}{2})}{\chi_2 \cos(\phi_2 + \frac{z}{2})} (2\eta_1)^{2\gamma} (2\eta)^{-2\gamma} \frac{1+f_2}{1+f_1} \frac{\Gamma(1+2\gamma)}{\Gamma(1+\gamma-i\frac{\alpha E}{k})} e^{-i\pi(\gamma+i\frac{\alpha E}{k})} + \frac{\Gamma(1-2\gamma)}{\Gamma(1-\gamma-i\frac{\alpha E}{k})} e^{-i\pi(-\gamma+i\frac{\alpha E}{k})}}, \quad (69)$$

where

$$f_1 \equiv \frac{\gamma + \frac{i\alpha E}{k}}{\nu - \frac{im\alpha}{k}}, \quad f_2 \equiv \frac{-\gamma + \frac{i\alpha E}{k}}{\nu - \frac{im\alpha}{k}}. \quad (70)$$

The expression in (69) gives the \mathbf{S} matrix for gapped graphene for the parameter range $0 < \gamma < \frac{1}{2}$. For this range of γ , the appropriate boundary conditions for which the Hamiltonian is self-adjoint and the corresponding time evolution is unitary, requires the introduction of an additional real self-adjoint extension parameter z , which labels the allowed boundary conditions. The phase shifts and the S matrix depend explicitly on z . For each value of z (mod 2π), we have an inequivalent set of the scattering data. Practically realizable value of z should be determined empirically as it cannot be determined analytically.

In Figure 7(a) we have shown the energy dependence of scattering phase shifts for three different values of the self adjoint extension parameter z . We can see from the Figure that the region $|E| < |m|$ is characterized by the sharp discontinuous oscillations which indicate the appearance of discrete bound states. In the other region where $|E| > |m|$, scattering phase shifts behave qualitatively in the same manner for different values of z but they are clearly distinguishable from each other. In Figure 7(b) we have observed the effect of topology on the energy dependence of scattering phase shifts for a particular self adjoint extension parameter. It should be noted that the Figure shows the effect of topology considering only two values of n ($n = 1, 3$) because the value of γ remains in the region $0 < \gamma < \frac{1}{2}$ for only those two values. During the analysis we have always restricted the obtained results to the parameter range $0 < \gamma < \frac{1}{2}$ through the appropriate choice of system parameters. In the plots we have assumed that $d = 1$.

In Figures 8(a) and 8(b) we have shown the dependence of LDOS on the distance r from the external Coulomb impurity placed at the apex of the gapped graphene cone where the energy is fixed at a value $E = 4m$. We have used the following expression given in equation Eq.(71) for LDOS during the plotting.

$$\mu(E, r) = \frac{4}{\pi\hbar v_F} \sum_j |\Psi^{(j)}(k, r)|^2. \quad (71)$$

For the numerical calculation we have used the Equations (11),(12), (63),(64) and (68). In Figures 8(c) and 8(d) we have plotted the energy dependence of LDOS at a distance close to the charge impurity ($r = 1$). From these Figures we can observe that LDOS depend on the values of self adjoint extension parameter z and also on the topology of the system. Therefore measurement of LDOS using scanning tunneling microscopy can give us information about the self adjoint extension parameter and the topology of the system.

IV. PROPERTIES OF GAPPED GRAPHENE CONE WITH SUPERCRITICAL COULOMB CHARGE

In the supercritical region the radial part of the Dirac equation obeyed by the gapped graphene cone appears to be the same as Eq.(13). The only difference is that in this region γ is always imaginary as the Coulomb potential strength α exceeds the value of ν . We denote $\gamma = i\lambda = \sqrt{\alpha^2 - \nu^2}$. Then from Eq.(13) we have

$$\rho \frac{dF}{d\rho} + (i\lambda - \frac{\alpha E}{\eta})F - (\nu + \frac{m\alpha}{\eta})G = 0, \quad (72)$$

and

$$\rho \frac{dG}{d\rho} + (i\lambda - \rho + \frac{\alpha E}{\eta})G + (-\nu + \frac{m\alpha}{\eta})F = 0. \quad (73)$$

Substituting the expression of G from Eq.(72) in Eq.(73) we have

$$\rho F'' + (1 + 2i\lambda - \rho)F' - (i\lambda - \frac{\alpha E}{\eta})F = 0. \quad (74)$$

Solving the differential equations we can obtain the low energy eigenstates of the gapped graphene cone using two different boundary conditions. In the next section we shall consider a regularized Coulomb potential and obtain the quasibound state energy spectrum and then we shall observe how the nonzero mass and cutoff parameter affects the critical charge of the system. We shall repeat the same calculations with the zigzag edge boundary condition also.

A. Regularized Coulomb Potential

In order to observe the supercritical effect of external Coulomb charge on the gapped graphene cone we shall first consider a regularized Coulomb potential because in that case we are allowed to extend the bound states until the negative continuum $E = -m$ is reached[58, 61]. The regularization of the Coulomb potential given by

$$V(r) = \begin{cases} -\alpha/r, & r > a \\ -\alpha/a, & r \leq a \end{cases}, \quad (75)$$

where the Coulomb charge is placed at the apex of the gapped graphene cone, a is the minimum distance of the Dirac electron from the apex and it is of the order of the lattice parameter. The Dirac equation for gapped graphene cone is solved for these two different regions.

Let us first consider the region $r \leq a$. In this region the Dirac equation is given by

$$\begin{pmatrix} (E - m + \frac{\alpha}{a}) & -\{\partial_r + (\nu + \frac{1}{2})\frac{1}{r}\} \\ \{\partial_r - (\nu - \frac{1}{2})\frac{1}{r}\} & (E + m + \frac{\alpha}{a}) \end{pmatrix} \begin{pmatrix} P_1^{(j)}(r) \\ Q_1^{(j)}(r) \end{pmatrix} = 0. \quad (76)$$

Eq. (76) gives the following two coupled first order differential equations.

$$-Q_1^{(j)}(r) - \frac{(\nu + \frac{1}{2})}{r}Q_1^{(j)}(r) + \left(E - m + \frac{\alpha}{a}\right)P_1^{(j)}(r) = 0 \quad (77)$$

and

$$P_1^{(j)}(r) - \frac{(\nu - \frac{1}{2})}{r}P_1^{(j)}(r) + \left(E + m + \frac{\alpha}{a}\right)Q_1^{(j)}(r) = 0. \quad (78)$$

Substituting the expression of $Q_1^{(j)}(r)$ from Equation (78) in Equation (77) we have

$$r^2 P_1''^{(j)}(r) + r P_1'^{(j)}(r) + \left[\left\{ \left(E + \frac{\alpha}{a}\right)^2 - m^2 \right\} r^2 - \left(\nu - \frac{1}{2}\right)^2 \right] = 0. \quad (79)$$

A general solution of this Bessel equation is given by

$$P_1^{(j)}(r) = A_1 J_{|\nu - \frac{1}{2}|} \left(r \sqrt{\left(E + \frac{\alpha}{a}\right)^2 - m^2} \right). \quad (80)$$

Using Eq. (80) we obtain

$$Q_1^{(j)}(r) = \sqrt{\frac{\left(E + \frac{\alpha}{a} - m\right)}{\left(E + \frac{\alpha}{a} + m\right)}} A_1 J_{|\nu + \frac{1}{2}|} \left(r \sqrt{\left(E + \frac{\alpha}{a}\right)^2 - m^2} \right). \quad (81)$$

Now we consider the region $r > a$. In this case the coupled 1st order differential equations and the second order differential equations obeyed by the Dirac fermions will be the same as Equations (72), (73) and (74). Then using the regularity condition at infinity we have [75]

$$F = U \left(i\lambda - \frac{E\alpha}{\eta}, 1 + 2i\lambda, \rho \right) \quad (82)$$

and

$$G = \left(\frac{m\alpha}{\eta} - \nu \right) U \left(1 + i\lambda - \frac{E\alpha}{\eta}, 1 + 2i\lambda, \rho \right). \quad (83)$$

Therefore the upper and lower components of the Dirac wave function will be given by

$$P_2^{(j)}(r) = \sqrt{m + E} e^{-\eta r} (2\eta r)^{(i\lambda - \frac{1}{2})} \left[U \left(i\lambda - \frac{E\alpha}{\eta}, 1 + 2i\lambda, \rho \right) + \left(\frac{m\alpha}{\eta} - \nu \right) U \left(1 + i\lambda - \frac{E\alpha}{\eta}, 1 + 2i\lambda, \rho \right) \right] \quad (84)$$

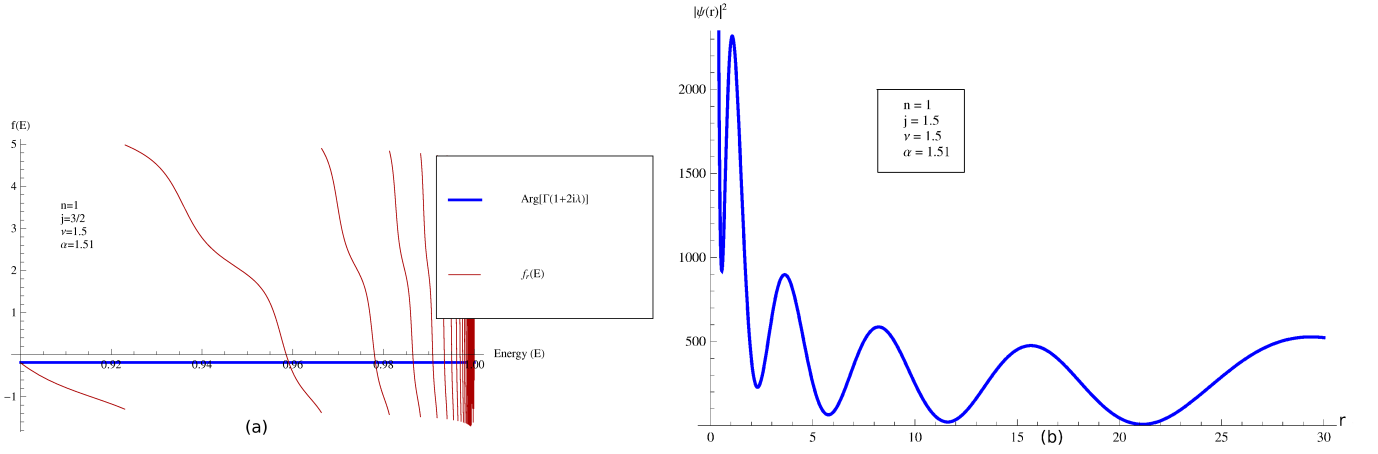


FIG. 6: (a) Bound state energy spectrum with regularized potential is shown. Here the blue line represents $\text{Arg}[\Gamma(1+2i\lambda)]$ and the dark red line represents RHS of Equation (89). (b) Dependence of $|\Psi(r)|^2$ on the distance r from the charge impurity placed at the apex of the gapped graphene cone is shown for a particular energy $E = 0.96m$ obtained from the plot of the bound state energy spectrum.

and

$$Q_2^{(j)}(r) = \sqrt{m-E} e^{-\eta r} (2\eta r)^{(i\lambda-\frac{1}{2})} \left[U\left(i\lambda - \frac{E\alpha}{\eta}, 1+2i\lambda, \rho\right) - \left(\frac{m\alpha}{\eta} - \nu\right) U\left(1+i\lambda - \frac{E\alpha}{\eta}, 1+2i\lambda, \rho\right) \right]. \quad (85)$$

To determine the bound states we use the continuity condition of the wave function at $r = a$. It is given by

$$\frac{P_1^{(j)}(r)}{Q_1^{(j)}(r)} \Big|_{r=a} = \frac{P_2^{(j)}(r)}{Q_2^{(j)}(r)} \Big|_{r=a}. \quad (86)$$

Using this condition given in Eq. (86) we have

$$\frac{U\left(i\lambda - \frac{E\alpha}{\eta}, 1+2i\lambda, 2\eta a\right)}{\left(\frac{m\alpha}{\eta} - \nu\right) U\left(1+i\lambda - \frac{E\alpha}{\eta}, 1+2i\lambda, 2\eta a\right)} = -\frac{\mu+1}{\mu-1} \quad (87)$$

where

$$\mu = \sqrt{\frac{(m+E)(E+\frac{\alpha}{a}-m)}{(m-E)(E+\frac{\alpha}{a}+m)}} \frac{J_{|\nu+\frac{1}{2}|}(\sqrt{(Ea+\alpha)^2-m^2a^2})}{J_{|\nu-\frac{1}{2}|}(\sqrt{(Ea+\alpha)^2-m^2a^2})}. \quad (88)$$

When $a \rightarrow 0$, the continuity condition given in Eq. (86) will be satisfied when

$$f(E) \equiv \frac{\Gamma(1+i\lambda - \frac{E\alpha}{\eta})}{\Gamma(1-i\lambda - \frac{E\alpha}{\eta})} e^{2i\lambda \ln(2\eta a)} \left[\frac{\nu - \frac{\alpha}{\eta}(m-E) + i\lambda}{\nu - \frac{\alpha}{\eta}(m-E) - i\lambda} \right] \left[\frac{\nu - \alpha \frac{J_{|\nu+\frac{1}{2}|}(\alpha)}{J_{|\nu-\frac{1}{2}|}(\alpha)} - i\lambda}{\nu - \alpha \frac{J_{|\nu+\frac{1}{2}|}(\alpha)}{J_{|\nu-\frac{1}{2}|}(\alpha)} + i\lambda} \right] = \frac{\Gamma(1+2i\lambda)}{\Gamma(1-2i\lambda)}$$

$$\text{or } f(E) \equiv f_r(E) = \text{Arg}[\Gamma(1+2i\lambda)]$$

(89)

where p is a positive integer and

$$f_r(E) = \text{Arg} \left[\Gamma \left(1 + i\lambda - \frac{E\alpha}{\eta} \right) \right] + \text{Arg} \left[\nu - \frac{\alpha}{\eta}(m-E) + i\lambda \right] + \lambda \ln(2\eta a) + \text{Arg} \left[\nu - \alpha \frac{J_{|\nu+\frac{1}{2}|}(\alpha)}{J_{|\nu-\frac{1}{2}|}(\alpha)} - i\lambda \right] + p\pi.$$

Eq. (89) gives the bound state energy spectrum in presence of a regularized Coulomb potential for all possible situations.

Now we concentrate to the physically interesting cases where $|E| \gg m$ and the Coulomb potential is near to its critical value i.e $\alpha \approx \alpha_c = |\nu_{\min}|$ for a particular n . Then from the Equation (89) we have

$$\ln \left(-2iE_p \sqrt{1 - \frac{m^2}{E_p^2} a} \right) = 2\psi(1) + \frac{J_{|\nu-\frac{1}{2}|}(\nu)}{\nu[J_{|\nu-\frac{1}{2}|}(\nu) - J_{|\nu+\frac{1}{2}|}(\nu)]} - \psi \left(1 - \frac{i\nu}{\sqrt{1 - \frac{m^2}{E_p^2}}} \right) - \frac{1}{\nu \left[1 + i\sqrt{\frac{1 - \frac{m}{E_p}}{1 + \frac{m}{E_p}}} \right]} - \frac{p\pi}{\lambda}. \quad (90)$$

Here $\psi(x) = \frac{\Gamma'(x)}{\Gamma(x)}$ and $\eta = -i\sqrt{E_p^2 - m^2}$. For $\frac{m}{E} \ll 1$ we have up to the terms of order $\frac{m^2}{E^2}$,

$$E_p - \frac{m^2}{2E_p} = \frac{1}{2a} \exp \left[\frac{J_{|\nu-\frac{1}{2}|}(\nu)}{\nu(J_{|\nu-\frac{1}{2}|}(\nu) - J_{|\nu+\frac{1}{2}|}(\nu))} + 2\psi(1) - \psi(1 - i\nu) - \frac{(1-i)}{2\nu} - \frac{p\pi}{\lambda} + \frac{i\pi}{2} \right] \left[1 - \frac{m}{E_p} \left(\frac{1}{2\nu} \right) + \frac{m^2}{E_p^2} \left\{ \frac{i\nu}{2} \psi'(1 - i\nu) - \frac{i}{4\nu} \right\} \right]. \quad (91)$$

Thus we can see the effect of the nonzero mass on the bound state energy spectrum.

The mass affects the critical charge of the system. For a regularized Coulomb potential the bound states can dive into negative energies. Here the critical charge refers to that value of Coulomb potential for which $E = -m$. Then for the region near critical potential we have

$$\alpha_c = \nu + \frac{\pi^2}{2\nu \log^2[2m\nu C a]} \quad (92)$$

where

$$C = \exp \left[-2\psi(1) - \frac{J_{|\nu-\frac{1}{2}|}(\nu)}{\nu(J_{|\nu-\frac{1}{2}|}(\nu) - J_{|\nu+\frac{1}{2}|}(\nu))} \right]. \quad (93)$$

From Equation (92) we can see when $ma \rightarrow 0$, $\alpha_c \approx \nu$ which agrees with the result obtained for massless case [76]. The dependence of critical charge on the nonzero mass and cutoff parameter are shown in Fig.(9) for different opening angles of the gapped graphene cone. From the Fig.(9) it is clear that the topology affects the critical charge of the system and the nature of their dependence on the product of mass and cutoff parameter of the system remains almost same.

B. Zigzag edge boundary condition

To find out the energies of the stationary states formed in the supercritical region now we use the zigzag edge boundary condition $\Psi_B^j(a) = 0$, where a is a distance from the apex, of the order of the lattice scale in graphene. In order to proceed we shall first solve Eq.(74) and obtain two linearly independent solutions $F_1(\rho)$ and $F_2(\rho)$ which are regular at $\rho = 0$. They are given by [75]

$$F_1(\rho) = A_1 M \left(i\lambda - \frac{E\alpha}{\eta}, 1 + 2i\lambda, \rho \right) \quad (94)$$

and

$$F_2(\rho) = A_2 \rho^{-2i\lambda} M \left(-i\lambda - \frac{E\alpha}{\eta}, 1 - 2i\lambda, \rho \right). \quad (95)$$

Then from Eq.(72) we have

$$G_1(\rho) = \frac{(i\lambda - \frac{\alpha E}{\eta})}{(\nu + \frac{m\alpha}{\eta})} A_1 M \left(1 + i\lambda - \frac{E\alpha}{\eta}, 1 + 2i\lambda, \rho \right) \quad (96)$$

and

$$G_2(\rho) = -\frac{(i\lambda + \frac{\alpha E}{\eta})}{(\nu + \frac{m\alpha}{\eta})} A_2 \rho^{-2i\lambda} M \left(1 - i\lambda - \frac{E\alpha}{\eta}, 1 - 2i\lambda, \rho \right). \quad (97)$$

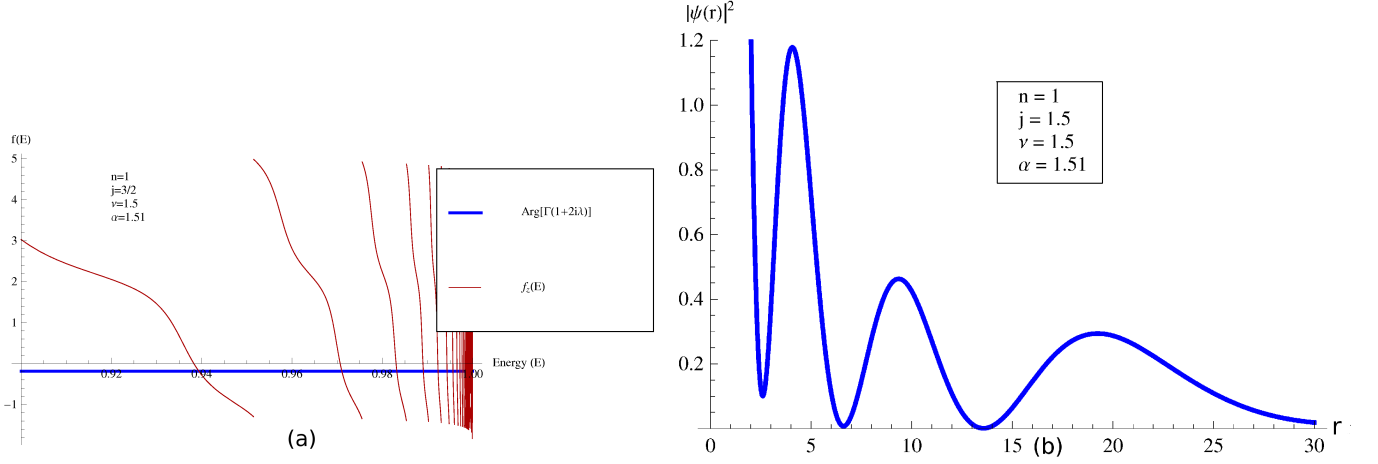


FIG. 7: (a) Bound state energy spectrum with zigzag edge boundary condition is shown. Here the blue line represents $\text{Arg}[\Gamma(1 + 2i\lambda)]$ and the red line represents RHS of Equation (100). (b) Dependence of $|\Psi(r)|^2$ on the distance r from the charge impurity placed at the apex of the gapped graphene cone is shown for a particular energy $E = 0.94m$ obtained from the plot of the bound state energy spectrum.

The solution satisfying the zigzag edge boundary condition can be given by

$$\Psi_B^j(r) = \sqrt{m - E} e^{-\frac{\rho}{2}} \rho^{\gamma - \frac{1}{2}} [\{F_1(a) - G_1(a)\}\{F_2(r) - G_2(r)\} - \{F_1(r) - G_1(r)\}\{F_2(a) - G_2(a)\}] \quad (98)$$

The square integrability condition of the wave function indicates that as $\rho \rightarrow \infty$ the diverging part of the wave function must vanish. Therefore we have

$$\sqrt{m - E} e^{\frac{\rho}{2}} \rho^{(-\frac{E\alpha}{\eta} - \frac{3}{2})} A_1 A_2 \left[\frac{\Gamma(1 - 2i\lambda)}{\Gamma(-i\lambda - \frac{E\alpha}{\eta})} \left\{ 1 - \frac{(i\lambda - \frac{E\alpha}{\eta})}{(\nu + \frac{m\alpha}{\eta})} \right\} - \frac{\Gamma(1 + 2i\lambda)}{\Gamma(i\lambda - \frac{E\alpha}{\eta})} \left\{ 1 - \frac{(-i\lambda - \frac{E\alpha}{\eta})}{(\nu + \frac{m\alpha}{\eta})} \right\} e^{-2i\lambda \ln(2\eta a)} \right] \left[1 - \frac{(\rho - 1 - \frac{2E\alpha}{\eta})}{(\nu + \frac{m\alpha}{\eta})} \right] = 0. \quad (99)$$

This gives the condition

$$\begin{aligned} \frac{\Gamma(1 - 2i\lambda)}{\Gamma(-i\lambda - \frac{E\alpha}{\eta})} \left\{ 1 - \frac{(i\lambda - \frac{E\alpha}{\eta})}{(\nu + \frac{m\alpha}{\eta})} \right\} &= \frac{\Gamma(1 + 2i\lambda)}{\Gamma(i\lambda - \frac{E\alpha}{\eta})} \left\{ 1 - \frac{(-i\lambda - \frac{E\alpha}{\eta})}{(\nu + \frac{m\alpha}{\eta})} \right\} e^{-2i\lambda \ln(2\eta a)} \\ \text{or } f(E) &\equiv \frac{\Gamma(i\lambda - \frac{E\alpha}{\eta})}{\Gamma(-i\lambda - \frac{E\alpha}{\eta})} e^{2i\lambda \ln(2\eta a)} \left[\frac{\nu + \frac{\alpha}{\eta}(m + E) - i\lambda}{\nu + \frac{\alpha}{\eta}(m + E) + i\lambda} \right] = \frac{\Gamma(1 + 2i\lambda)}{\Gamma(1 - 2i\lambda)} \\ \text{or } f(E) &\equiv f_z(E) = \text{Arg}[\Gamma(1 + 2i\lambda)] \end{aligned} \quad (100)$$

where p is a positive integer and

$$f_z(E) = \text{Arg} \left[\Gamma \left(i\lambda - \frac{E\alpha}{\eta} \right) \right] + \text{Arg} \left[\nu + \frac{\alpha}{\eta}(m + E) - i\lambda \right] + \lambda \ln(2\eta a) + p\pi.$$

This is the condition directly obtained from our analysis and obeyed by the bound state energy spectrum for all possible situations.

We can compare this bound state energy spectrum for zigzag edge boundary with the spectrum obtained from the regularized potential case and observe how the two different boundary conditions affect the spectrum. From Fig.(8) we can observe that the bound state energy spectra and the probability amplitude of the wavefunction gets affected by the boundary conditions though their nature remains same.

Now we again concentrate to some physically interesting cases with some approximations. First we consider the case where $|E| \gg m$ and the Coulomb potential is near to its critical value i.e $\alpha \approx \alpha_c = |\nu_{\min}|$ for a particular n .

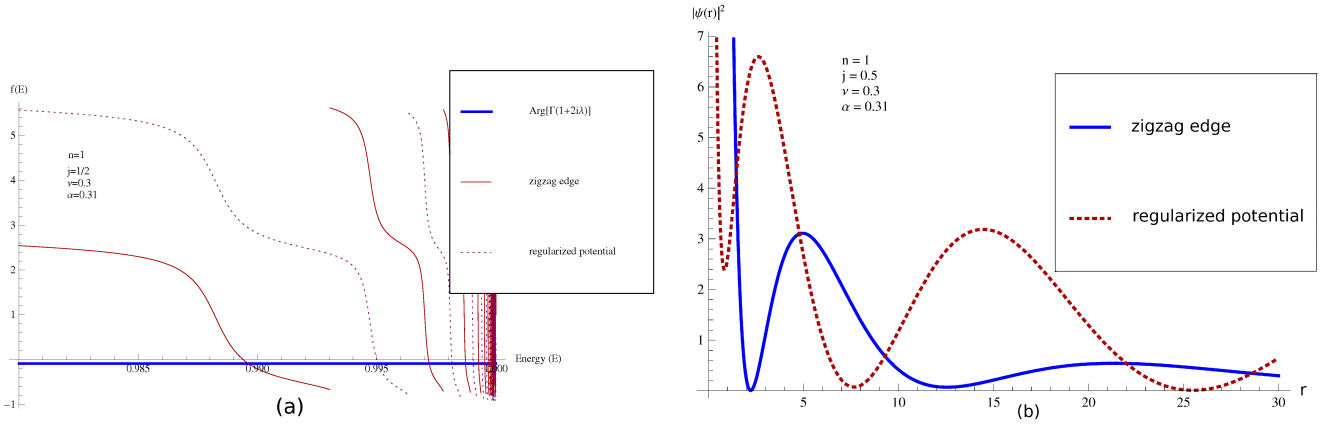


FIG. 8: (a) Bound state energy spectrum with zigzag edge boundary condition and regularized Coulomb potential. Here the blue line represents $\text{Arg}[\Gamma(1+2i\lambda)]$ and the dashed and the solid line represents RHS of Equations (100) and (89) respectively. (b) Dependence of $|\Psi(r)|^2$ on the distance r from the charge impurity placed at the apex of the gapped graphene cone is shown for both the zigzag edge boundary condition and regularized Coulomb potential. The values of energy are obtained from the bound state energy spectrum. From Fig.(a) we can see that for zigzag edge boundary condition a possible bound state energy is $E = 0.9895m$ and for regularized potential a possible energy is $E = 0.995m$. Here we have given the probability amplitude plots for these two particular energies.

Then from the Equation (100) we have

$$\ln \left(-2iE_p \sqrt{1 - \frac{m^2}{E_p^2}} a \right) = 2\psi(1) - \psi \left(-\frac{i\nu}{\sqrt{1 - \frac{m^2}{E_p^2}}} \right) + \frac{1}{\nu \left[1 + i\sqrt{\frac{1 + \frac{m}{E_p}}{1 - \frac{m}{E_p}}} \right]} - \frac{p\pi}{\lambda}. \quad (101)$$

Like the previous section here also $\psi(x) = \frac{\Gamma'(x)}{\Gamma(x)}$ and $\eta = -i\sqrt{E_p^2 - m^2}$. For $\frac{m}{E} \ll 1$ we have up to the terms of order $\frac{m^2}{E^2}$,

$$E_p - \frac{m^2}{2E_p} = \frac{1}{2a} \exp \left[\left\{ 2\psi(1) - \psi(-i\nu) + \frac{(1-i)}{2\nu} - \frac{p\pi}{\lambda} \right\} - \frac{m}{E_p} \left(\frac{1}{2\nu} \right) + \frac{m^2}{E_p^2} \left\{ \frac{i\nu}{2} \psi'(-i\nu) + \frac{i}{4\nu} \right\} \right]$$

or $E_p - \frac{m^2}{2E_p} = \frac{1}{2a} \exp \left[2\psi(1) - \psi(-i\nu) + \frac{(1-i)}{2\nu} - \frac{p\pi}{\lambda} \right] \left[1 - \frac{m}{E_p} \left(\frac{1}{2\nu} \right) + \frac{m^2}{E_p^2} \left\{ \frac{i\nu}{2} \psi'(-i\nu) + \frac{i}{4\nu} \right\} \right]. \quad (102)$

Thus we can see the effect of the nonzero mass on the bound state energy spectrum.

Like the critical charge obtained for regularized Coulomb potential, here also with zigzag edge boundary condition we can see that the mass affects the critical charge of the system. Proceeding as before in this case we have

$$\alpha_c = \nu + \frac{\pi^2}{2\nu \log^2 [2m\nu a \exp(-2\psi(1))]}. \quad (103)$$

Here also from Equation (103) we can see when $ma \rightarrow 0$, $\alpha_c \approx \nu$ which agrees with the result obtained for massless case [76]. The dependence of critical charge on the nonzero mass and cutoff parameter has been shown for different opening angles of the gapped graphene cone. Also we have compared the dependence for two different boundary conditions.

From Fig.(9) we can see that for a zigzag edge boundary condition the critical charge vary with ma more rapidly than it varies for a regularized Coulomb potential. Thus the two different boundary conditions affect the dependence of critical charge of a gapped graphene cone on ma .

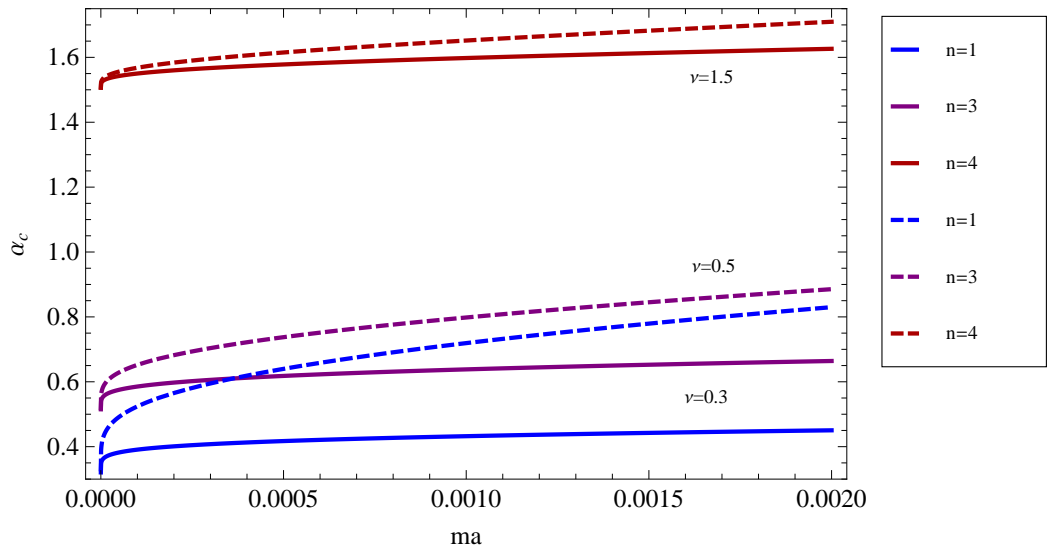


FIG. 9: Dependence of critical charge on the nonzero mass and cutoff parameter are shown for both zigzag edge boundary condition and regularized Coulomb potential for different opening angles of the gapped graphene cone. The dotted lines show the dependence for zigzag edge boundary condition and the solid lines show the dependence for regularized Coulomb potential

V. CONCLUSION

In this paper we have described the low energy dynamics of massive Dirac fermions in a gapped graphene cone in the presence of an external Coulomb charge impurity. The graphene cone can be equivalently described as a graphene plane together with a flux tube whose gauge potential is chosen to produce the required holonomies. The given system thus consists of a gapped graphene plane together with a combination of a Coulomb charge impurity and a flux tube passing through it. The strength of the Coulomb charge can be sub or supercritical.

The combination of this topological defect as well as the charge impurity results in short distance interactions, the effect of which cannot be incorporated as dynamical terms in the Dirac equation, valid in the low energy limit. For a sub critical charge impurity, we show that the effect of these interactions can be modelled through appropriate choice of boundary conditions, which are determined by imposing the requirement of a unitary time evolution. While there is a very large class of allowed boundary conditions, it turns out that they can be labelled by a single real parameter. It is this parameter through which the effect of the short range interactions enter in the analysis presented here. This parameter cannot be determined from theory alone. However, we have shown that the observables such as LDOS, scattering phase shifts and bound state energies depend explicitly on this parameter. As mentioned before, a similar situation arose in the context of Dirac fermions in a plane in the presence of a cosmic string. These two situations are not identical, but similar quantum subtleties arise in both contexts and the case of the gapped graphene considered here is more amenable to empirical analysis.

The supercritical regime of the external Coulomb charge is characterized by quantum instabilities. Here we have analyzed the effect of topological defects in the supercritical dynamics of gapped graphene. This problem has been analyzed with a regularized Coulomb potential as well as with a zigzag boundary condition. We have shown that the quasibound state spectra and the probability amplitude depend explicitly on the number of sectors removed from a planar graphene to form the cone. In addition, the running of the critical charge as a function of the product of the Dirac mass m and the cutoff parameter a has been obtained. Though the nature of the dependence is similar for both the regularized Coulomb potential and the zigzag boundary condition but in the latter case the critical charge increases more rapidly with ma than the former case.

It would be interesting to study the effect of sample topology on the electron-electron interactions in graphene and the associated gap equation, which is currently under investigation.

[1] P. de Sousa Gerbert and R. Jackiw, Commun. Math. Phys. **124**, 229-260 (1989).

[2] P. de Sousa Gerbert. Phys. rev. **D 40**, 1346 (1989).

- [3] K. S. Novoselov, A. K. Geim, S. V. Morozov, D. Jiang, M. I. Katsnelson, I. V. Grigorieva and A. A. Firsov, *Science* **306**, 666 (2004).
- [4] K. S. Novoselov, A. K. Geim, S. V. Morozov, D. Jiang, M. I. Katsnelson, I. V. Grigorieva, S. V. Dubonos and A. A. Firsov, *Nature* **438**, 197 (2005).
- [5] Y. Zhang, Y.-W. Tan, H. L. Stormer and P. Kim, *Nature* **438**, 201 (2005).
- [6] Wallace, P. R. The band theory of graphite. *Phys. Rev.* **71**, 622 (1947).
- [7] D. P. DiVincenzo and E. J. Mele, *Phys. Rev.* **B 29**, 1685 (1984).
- [8] G. W. Semenoff, *Phys. Rev. Lett.* **53**, 2449 (1984).
- [9] A. K. Geim and K.S. Novoselov, *Nature Materials* **6**, 183 (2007).
- [10] A.H.Castro Neto, F.Guinea, N.M.R. Peres, K.S. Novoselov and A.K.Geim, *Rev. Mod. Phys.* **81**, 109 (2009).
- [11] N. M. R. Peres, *Rev. Mod. Phys.* **82**, 2673 (2010).
- [12] S. Das Sarma, Shaffique Adam, E. H. Hwang, Enrico Rossi, *Rev. Mod. Phys.* **83**, 407 (2011).
- [13] J.Gonzalez, F. Guinea and M.A.H.Vozmediano, *Phys. Rev. Lett.* **69**, 172 (1992).
- [14] J. Gonzalez, F. Guinea and M.A.H.Vozmediano, *Nucl. Phys.B* **406**, 771 (1993).
- [15] P.E. Lammert, V.H. Crespi, *Phys. Rev. Lett.* **85**, 5190 (2000).
- [16] P.E. Lammert, V.H. Crespi, *Phys. Rev. B* **69**, 035406 (2004).
- [17] D. V. Kolesnikov and V. A. Osipov, *Eur. Phys. J. B* **49**, 465 (2006).
- [18] Yurii A Sitenko and Nadiia D Vlasii, *Nuclear Physics B* **787**, 241, (2007).
- [19] A.Cortijo, M.A.H.Vozmediano, *Nucl. Phys.B* **763**, 293 (2007).
- [20] F.de Juan, A. Cortijo and M.A.H.Vozmediano, *Phys. Rev. B* **76**, 165409 (2007).
- [21] Hou C-Y, C. Chamon and C. Mudry, *Phys. Rev. Lett.* **98**, 186809 (2007).
- [22] J. Pachos, M. Stone and K.Temme, *Phys. Rev. Lett.* **100**, 156806 (2008).
- [23] C.Furtado, F.Moraes, A.M. de M. Carvalho, *Phys. Lett. A* **372**, 5368 (2008).
- [24] A. Roy and M. Stone, *J. Phys. A* **43**, 015203 (2010).
- [25] M.A.H.Vozmediano, M.I.Katsnelson and F. Guinea, *Phys. Reports* 493 (2010).
- [26] J. Gonzalez, J.Herrero, *Nucl. Phys. B* **825**, 426 (2010).
- [27] O. V. Yazyev, S. G. Louie *Phys. Rev. B* **81**, 195420 (2010).
- [28] J. M. Fonseca, W. A. Moura-Melo, A. R. Pereira, *Phys. Lett. A*, **374**, 4359 (2010).
- [29] F. de Juan, A. Cortijo, M. A. H. Vozmediano and A. Cano, *Nature Physics* **7**, 810 (2011).
- [30] A. Cortijo, F. Guinea and M.A.H.Vozmediano, arXiv:1112.2054 (2011).
- [31] N. Abedpour, R. Asgari and F.Guinea, *Phys. Rev. B* **84**, 115437 (2011).
- [32] K. Bakke, A.Yu. Petrov, C. Furtado, arXiv:1111.0836.
- [33] E.V. Gorbar, V.P. Gusynin, V.A. Miransky and I.A. Shovkovy, *Phys. Rev. B* **66**, 045108 (2002).
- [34] D.V.Khveshchenko, H.Leal. *Nucl. Phys. B* **687**, 323 (2004).
- [35] C.L.Kane and E.J.Mele, *Phys. Rev. Lett.* **95**, 226801 (2005).
- [36] D. S. Novikov, *Phys. Rev. B* **76**, 245435 (2007).
- [37] V. P. Gusynin, V. A. Miransky, S. G. Sharapov and I. A. Shovkovy, *Phys. Rev. B* **77**, 205409 (2008).
- [38] D.V.Khveshchenko, *J.Phys.:Condens. Matter* **21**, 075303 (2009).
- [39] O.V.Gamayun, E.V.Gorbar and V.P.Gusynin, *Phys. Rev. B* **81**, 075429 (2010).
- [40] Wei Li, Guo-Zhu Liu. *Phys. Lett. A* **374**, 2957 (2010).
- [41] Y. Araki and Tetsuo Hatsuda, *Phys. Rev. B* **82**, 121403 (R) (2010).
- [42] Y. Araki, *Journal of Physics : Conference Series* **302**, 012022 (2011).
- [43] J. L. Zhu, S. Sun, N. Yang, *Phys. Rev. B* **85**, 035429 (2012).
- [44] M.Y. Han et al. *Phys. Rev. Lett.* **98**, 206805 (2007).
- [45] S.Y. Zhou et al. *Nat. Mater.* **6**, 770 (2007).
- [46] S.Y. Zhou et al. *Nat. Mater.* **7**, 259 (2008).
- [47] D. Haberer et al. *Nano Letters*, **10**, 3360 (2010).
- [48] D.R.Cooper et al. *ISRN Condensed Matter Physics*, Vol 2012, 501686.
- [49] Eva Y Andrei et al. *Rep. Prog. Phys.* **75** 056501 (2012).
- [50] Dong -Keun Ki, A.F. Morpurgo, arXiv:1203.0540 (accepted at *Phys. Rev. Lett.*).
- [51] J. Reinhardt and W. Greiner, *Rep. Prog. Phys.* **40**, 219 (1977).
- [52] W. Greiner, B. Muller, and J. Rafelski, *Quantum Electrodynamics of Strong Fields* (Springer-Verlag, Berlin, 1985).
- [53] M. I. Katsnelson, K. S. Novoselov and A. K. Geim, *Nature Physics* **2**, 620 (2006).
- [54] M.I.Katsnelson and K.S. Novoselov, *Solid State Communications*, Volume **143**, Issues 1-2, July 2007, Pages 3-13.
- [55] V. M. Pereira, J. Nilsson and A. H. Castro Neto, *Phys. Rev. Lett.* **99**, 166802 (2007).
- [56] A. V. Shytov, M. I. Katsnelson and L. S. Levitov, *Phys. Rev. Lett.* **99**, 236801 (2007).
- [57] A. V. Shytov, M. I. Katsnelson and L. S. Levitov, *Phys. Rev. Lett.* **99**, 246802 (2007).
- [58] V. M. Pereira, V.N.Kotov and A. H. Castro Neto, *Phys. Rev. B* **78**, 085101 (2008).
- [59] A. Shytov, M. Rudner, N. Gu, M. Katsnelson and L. levitov, *Solid State Comm.* **149**, 1087 (2009).
- [60] Kumar S. Gupta and Siddhartha Sen, *Mod. Phys. Lett. A* **24**, 99 (2009).
- [61] O.V.Gamayun, E.V.Gorbar and V.P.Gusynin, *Phys. Rev. B* **80**, 165429 (2009).
- [62] A.I.Milstein, I.S.Terekhov. *Phys. Rev. B* **81**, 125419 (2010).
- [63] J. Wang, H. A. Fertig and Ganpathy Murthy, *Phys. Rev. Lett.* **104**, 186401(2010).
- [64] O.V.Gamayun, E.V.Gorbar and V.P.Gusynin, *Phys. Rev. B* **83**, 235104 (2011).

- [65] V.N.Kotov, B. Uchoa, V.M.Pereira, F.Guinea, A. H. Castro Neto, Rev. Mod. Phys. 84, 1067 (2012).
- [66] H.Yamagishi, Phys. Rev. D **27** 2383 (1983).
- [67] R. Jackiw and S.Y. Pi, Phys. Rev. Lett. **98**, 266402 (2007).
- [68] C. Chamon, C. Y. Hou, R. Jackiw, C. Mudry, S. Y. Pi and G. Semenoff, Phys.Rev. B **77**, 235431 (2008).
- [69] R. Jackiw and S.Y. Pi, Phys. Rev. B **78**, 132104 (2008).
- [70] R. Jackiw, A.I.Milstein, S.Y. Pi and I.S.Terekov, Phys. Rev. B **80**, 033413 (2009).
- [71] M. Reed and B. Simon, *Methods of Modern Mathematical Physics*, volume 2, (Academic Press, New York, 1972).
- [72] H. Falomir and P.A.G. Pisani, J. Phys. A : Math. Gen. **34**, 4143 (2001).
- [73] Kumar S. Gupta and Siddhartha Sen, Phys. Rev. B **78**, 205429 (2008).
- [74] K. S. Gupta, A.Samsarov and S. Sen, Eur. Phys. J. B **73** 389 (2010).
- [75] M. Abramowitz and I.A. Stegun, *Handbook of Mathematical Functions* (Dover, New York, 1970).
- [76] B. Chakraborty, Kumar S.Gupta and Sidhdhartha Sen, Phys. Rev. B **83**, 115412 (2011).